PAPER • OPEN ACCESS

Extreme-value statistics of stochastic transport processes

New Journal of Physics
The open access journal at the forefront of physics

Deutsche Physikalische Gesellschaft DPG
IOP Institute of Physics

Published in partnership with: Deutsche Physikalische Gesellschaft and the Institute of Physics

OPEN ACCESS

RECEIVED
21 August 2020

REVISED
13 November 2020

ACCEPTED FOR PUBLICATION
1 December 2020

PUBLISHED
23 December 2020

PAPER

Extreme-value statistics of stochastic transport processes

Alexandre Guillet[1,3], **Edgar Roldán**[2,*] and **Frank Jülicher**[3,*]

[1] Univ. Bordeaux, CNRS, LOMA, UMR 5798, F-33400 Talence, France
[2] ICTP-The Abdus Salam International Centre for Theoretical Physics, Strada Costiera 11, 34151, Trieste, Italy
[3] Max Planck Institute for the Physics of Complex Systems, Nöthnizer Strasse 38, 01187 Dresden, Germany
[*] Authors to whom any correspondence should be addressed.

E-mail: edgar@ictp.it and julicher@pks.mpg.de

Keywords: stochastic thermodynamics, molecular motors, extreme values, random matrix theory, relaxation phenomena

Abstract

We derive exact expressions for the finite-time statistics of extrema (maximum and minimum) of the spatial displacement and the fluctuating entropy flow of biased random walks. Our approach captures key features of extreme events in molecular motor motion along linear filaments. For one-dimensional biased random walks, we derive exact results which tighten bounds for entropy production extrema obtained with martingale theory and reveal a symmetry between the distribution of the maxima and minima of entropy production. Furthermore, we show that the relaxation spectrum of the full generating function, and hence of any moment, of the finite-time extrema distributions can be written in terms of the Marčenko–Pastur distribution of random-matrix theory. Using this result, we obtain efficient estimates for the extreme-value statistics of stochastic transport processes from the eigenvalue distributions of suitable Wishart and Laguerre random matrices. We confirm our results with numerical simulations of stochastic models of molecular motors.

1. Introduction

Life is a non-equilibrium phenomenon characterized by fluxes of energy and matter at different scales. At the molecular level, molecular motors play a key role for the generation of movements and forces in cells. Examples are vesicle transport, muscle contraction, cell division and cell locomotion [1, 2]. A molecular motor consumes a chemical fuel, adenosine triphosphate (ATP), that is hydrolysed to adenosine diphosphate (ADP) and inorganic phosphate. The chemical energy of this reaction is transduced to generate spontaneous movements and mechanical work. Single-molecule experiments have revealed that the activity of single or a few molecular motors displays strong fluctuations [3–13] which can be captured by the theory of stochastic processes [14–21].

An important question is to understand general features and universal properties that govern the statistics of fluctuations of stochastic transport processes that include the motion of molecular motors. Universal relations for the fixed-time statistics of time-integrated currents, such as the distance travelled and the work performed, have been investigated in the framework of non-equilibrium stochastic thermodynamics [22–25]. These results provide e.g. universal bounds for the efficiency of molecular motors given by the ratio between the mechanical power and the chemical power put in the motor [26]. Timing statistics of enzymatic reactions, such as those powering the motion of molecular motors, have been discussed within the framework of Kramers theory [27]. Recent theory and experiments in Kinesin have revealed symmetry relations between forward and backward cycle-time distributions of enzymatic reactions [28–30]. Related results have been derived in the context of waiting times of active molecular processes [31] and transition-path times in folding transitions of DNA hairpins [32].

When discussing stochastic processes, it is often sufficient to study averages and small fluctuations. However, rare events and large fluctuations play an important role when resilience and reliability of a system are investigated. In this context, the statistics of extreme values and of extreme excursions from the average play an important role, as has been discussed applying extreme-value theory in biophysics [33–35]

but also in other fields ranging from statistical physics [36] to climate [37, 38], finance [39–41], and sports [42–44].

Extreme events are important in biophysics as they are key to understand the robustness of biological processes. Illustrating examples are microtubule catastrophes or a sperm winning a race against a billion competitors. Here we consider the extreme value statistics of transport processes. Extreme-value theory has provided useful insights for e.g. long-range correlations of DNA sequences [33, 34] and DNA replication statistics in frogs' embryonic cells [35]. However, exact results on extreme-value statistics of stochastic transport phenomena in biophysics at finite time are so far lacking. For example, what is the maximal excursion of a molecular motor against or in the average direction of its motion within a given time? How long does it take a motor to reach its maximum excursion against the chemical bias? What is the entropy production associated with an extreme fluctuation of a molecular motor?

The statistics of extreme values of random walks has raised a lot of interest. In particular the record statistics of correlated time series was investigated in the long-time limit [36, 45–51]. These results also apply to continuous-time random walks in the long time limit [49] and to biased diffusions [48], for which exact results can be obtained also at finite time [31, 52]. However, the extrema statistics of biased hopping processes such as the transport of molecular motors is not captured by these results, except for the limit of weak bias. Recently, exploiting the duality between extreme values and first-passage times, it was shown for Markov processes in confining potentials that extreme values behave as a relaxation process with a discrete relaxation spectrum [53–55]. It remains an open question to understand the generic features of the relaxation spectra of the time dependent extreme value statistics of stochastic processes.

In this article, we derive exact results for extreme-value statistics of a simple and generic model of stochastic transport. We discuss the statistics of the maximum and minimum excursion (with respect to its initial location) and the associated extremal entropy changes. Moreover, we investigate the timescales associated with those extrema, combining concepts from stochastic thermodynamics, random walks and random-matrix theory. As we show below, our results provide insights on extreme-value statistics beyond recently derived inequalities for the finite-time infimum statistics of entropy production [31, 56]. We show that this finite-time statistics of entropy-production extrema can be written in terms of a continuous relaxation spectrum with finite support. Strikingly, this spectrum is known as the Marčenko–Pastur distribution, revealing a connection between relaxation of finite-time extrema statistics and random matrix theory. We then illustrate the results of our theory by constructing efficient random-matrix estimates for extrema, and apply them in the context of molecular motors.

The article is organized as follows: section 2 describes the model of stochastic transport used in this paper and provides exact extreme-value statistics for one dimensional (1D) biased random walks. Section 3 discusses the connection between extrema of 1D biased random walks and random matrix theory. In section 4 we apply our theory to two-dimensional stochastic models of molecular motors. Section 5 concludes the paper. Details on the derivations and numerical simulations are provided in the appendices.

2. Extreme-value statistics of 1D biased random walks

Many nonequilibrium phenomena at mesoscales can be described at a coarse-grained level as a continuous-time Markov jump process between discrete states x, y, z etc, with exponential waiting times. The transition rate from x to y can be written as [57–59]

$$k(x,y) = \nu(x,y)\mathrm{e}^{A(x,y)/2}, \tag{1}$$

with $\nu(x,y) = \nu(y,x)$ symmetric and $A(x,y) = -A(y,x)$ antisymmetric with respect to the exchange $x \to y$. If local detailed balance holds $A(x,y) = \beta[W(x) - W(y)]$ with $W(x)$ the potential energy of state x, $\beta = (k_\mathrm{B}T)^{-1}$ with k_B Boltzmann's constant and T the temperature of a thermostat. First, we consider the simple case of a 1D biased random walk on a line with discrete states denoted by the integer $x \in \mathbb{Z}$ (see figure 1(a) for an illustration). The forward and backward jump rates are given by $k_\pm \equiv k(x, x \pm 1) = \nu \mathrm{e}^{\pm A/2}$. Here $\nu > 0$ is a rate and $A > 0$ the affinity, which satisfy

$$\nu = \sqrt{k_+ k_-}, \qquad A = \ln(k_+/k_-). \tag{2}$$

This biased random walk describes e.g. the motion of a molecular motor along a periodic track fuelled by ATP [19]. In the simplest case, $A = \beta\Delta\mu$, with $\Delta\mu = \mu_\mathrm{ATP} - (\mu_\mathrm{ADP} + \mu_\mathrm{P})$ the chemical potential difference of ATP hydrolysis, often of the order of $20k_\mathrm{B}T$, and the rate ν depends on ATP concentration and internal timescales that determine the dwell-time statistics of the motor.

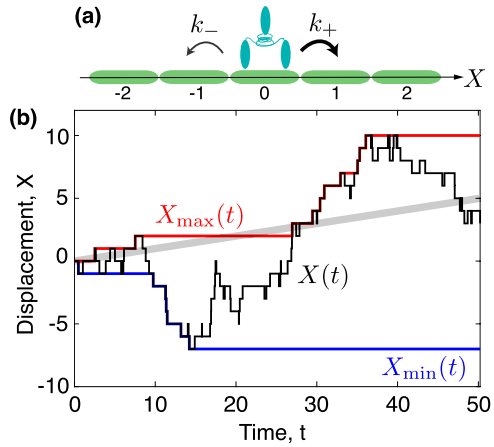

Figure 1. (a) Sketch of a one-dimensional (1D) biased random walk with hopping rates k_+ and k_- with displacement X. (b) Example of a trajectory $X(t)$ (black), its maximum $X_{\max}(t)$ (red), minimum $X_{\min}(t)$ (blue) and its average over many realizations $\langle X(t)\rangle$ (thick grey) as a function of time t. The trajectories are obtained from a numerical simulation of a 1D biased random walk with hopping rates $k_+ = 1.05$ and $k_- = 0.95$ in the positive and negative direction, respectively. The entropy production along the trajectory $X(t)$ is $S(t) = AX(t)$, with $A = \ln(k_+/k_-) = 0.1$.

An individual trajectory of a motor starting from a reference state $X(0) = 0$ at time $t = 0$ is denoted by $X_{[0,t]} = \{X(s)\}_{s=0}^{t}$. It contains jumps $j = 1, 2, \ldots$ from state x_j^- to state x_j^+ that occur at stochastic times t_j. The entropy production in unit of k_B associated with this trajectory is $S(t) = \ln[\mathcal{P}(X_{[0,t]})/\mathcal{P}(\tilde{X}_{[0,t]})] = AX(t)$ [31]. Here $\mathcal{P}$ is the path probability and $\tilde{X}_{[0,t]} = \{X(t-s)\}_{s=0}^{t}$ is the time reversed path. Thus, the entropy production $S(t)$ is a stochastic variable that undergoes a biased random walk of step size A with trajectories $S_{[0,t]} = AX_{[0,t]}$. For A positive, both the average velocity $v = \langle X(t)\rangle/t = (k_+ - k_-) = 2\nu \sinh(A/2)$ and the average rate of entropy production $\sigma = \langle S(t)\rangle/t = vA$ are positive. Here and in the following we denote by $\langle\cdot\rangle$ averages over many realizations of the process $X(t)$. However, due to fluctuations, the stochastic variables $X(t)$ and $S(t)$ can in principle take any value with finite probability and even become negative.

We now derive exact expressions for the statistics of the minimum $X_{\min}(t) = \min_{\tau\in[0,t]} X(\tau)$ and the maximum $X_{\max}(t) = \max_{\tau\in[0,t]} X(\tau)$ of the position of the motor with respect to its initial position, see figure 1(b) for illustrations. We also discuss the global minimum and maximum of the stochastic entropy production $S(t) = AX(t)$ denoted by $S_{\min}(t)$ and $S_{\max}(t)$, respectively. We first discuss the statistics of the global extrema of the position $X_{\min} \equiv \lim_{t\to\infty} X_{\min}(t)$ and $X_{\max} \equiv \lim_{t\to\infty} X_{\max}(t)$, and of the entropy production, $S_{\min}$ and $S_{\max}$. The probability that the global minimum of the discrete position is $-x$, with $x \geqslant 0$, is $P(X_{\min} = -x) = P_{\rm abs}(-x) - P_{\rm abs}(-x-1)$, where $P_{\rm abs}(-x) = \mathrm{e}^{-Ax}$ [31] is the probability that $X(t)$ reaches an absorbing site in $-x$ at a finite time. Thus, the global minimum follows a geometric distribution

$$P(X_{\min} = -x) = P(S_{\min} = -Ax) = \mathrm{e}^{-Ax}(1 - \mathrm{e}^{-A}), \tag{3}$$

for $x \geqslant 0$ and $P(X_{\min} = x) = P(S_{\min} = Ax) = 0$ for $x < 0$. From equation (3) we obtain the mean global minimum of a 1D biased random walk and of its associated entropy production:

$$\langle X_{\min}\rangle = \frac{-1}{\mathrm{e}^A - 1}, \qquad \langle S_{\min}\rangle = \frac{-A}{\mathrm{e}^A - 1}. \tag{4}$$

Therefore, the global minimum of the position diverges in the limit of a small bias A whereas the entropy production minimum is bounded for all $A \geqslant 0$ and obeys the infimum law $\langle S_{\min}\rangle \geqslant -1$ [31]. This bound is saturated in the limit of small affinity, which corresponds to the diffusion limit [60]. Because $S(t)$ and $X(t)$ have positive drift, the average global maxima of entropy production and displacement are not defined. However the difference $\lim_{t\to\infty}[\langle S_{\max}(t)\rangle - \langle S(t)\rangle] = A/(\mathrm{e}^A - 1)$ is finite and obeys symmetry properties that we discuss below.

Finite-time extrema statistics of the 1D biased random walk may be obtained from the finite-time absorption probabilities

$$\begin{aligned} P(X_{\min}(t) = -x) &= P(S_{\min}(t) = -Ax) \\ &= P_{\rm abs}(-x; t) - P_{\rm abs}(-x-1; t), \end{aligned} \tag{5}$$

where $P_{\rm abs}(-x;t)$ is the probability that X reaches an absorbing site at $-x$ at any time smaller than or equal to t. The absorption probability $P_{\rm abs}(x;t)=\delta_{x,0}+\int_0^t P_{\rm fpt}(T;x){\rm d}T$, with $\delta_{i,j}$ Kronecker's delta and

$$P_{\rm fpt}(T;x)={\rm e}^{Ax/2}\frac{|x|}{T}I_x(2\nu T){\rm e}^{-2\nu\,\cosh(A/2)T}, \tag{6}$$

is the first-passage time probability for the walker to first reach an absorbing site in x, with $|x|\geqslant 1$, at time $T\geqslant 0$ [61, 62], see appendix A. Here I_x denotes the xth order modified Bessel function of the first kind. Note that $\int_0^\infty {\rm d}T\; P_{\rm fpt}(T;x)=P_{\rm abs}(x)\leqslant 1$. We identify in equation (6) two timescales. The smaller timescale $\tau_1=(k_++k_-)^{-1}=(2\nu\;\cosh(A/2))^{-1}$ is the average waiting time between two jumps, and $\tau_2=(2\sqrt{k_+k_-})^{-1}=(2\nu)^{-1}$ is inversely proportional to the geometric mean of the transition rates; their ratio $\tau_2/\tau_1=\cosh(A/2)\geqslant 1$ increases with the bias strength. Normalizing (6) by $P_{\rm abs}(x)$, we obtain the mean $\langle T\rangle=|x|A/\sigma$ and variance ${\rm Var}[T]=(\coth(A/2)/|x|)\langle T\rangle^2$ of the first-passage time, in agreement with the first-passage time uncertainty relation ${\rm Var}[T]/\langle T\rangle\geqslant 2/\sigma$ [63]. Furthermore, the first-passage time probability density (6) obeys the following symmetry properties. First, the ratio

$$\frac{P_{\rm fpt}(T;x)}{P_{\rm fpt}(T;-x)}={\rm e}^{Ax}, \tag{7}$$

is independent on T, as follows from the stopping-time fluctuation theorem [28, 31, 64]. Second, the 'conjugate' first-passage time probability $\tilde{P}_{\rm fpt}(T;x)$, obtained exchanging k_+ by k_- (i.e. A by $-A$), obeys

$$\frac{P_{\rm fpt}(T;x)}{\tilde{P}_{\rm fpt}(T;x)}={\rm e}^{Ax}. \tag{8}$$

These two properties imply $\tilde{P}_{\rm fpt}(T;x)=P_{\rm fpt}(T;-x)$, which has interesting consequences for random walks [48, 65] and for the extrema statistics of $S(t)$, see below.

In order to derive exact finite-time extrema statistics, it is often convenient to use generating functions and Laplace transforms. The generating functions of the distributions of finite-time entropy production extrema are defined as $G_{\rm min/max}(z;t)=\sum_{x=-\infty}^{\infty}z^xP\left(S_{\rm min/max}(t)=Ax\right)\Theta(\mp x)$, with Θ the Heaviside function. Their Laplace transforms are given by $\hat{G}_{\rm min/max}(z;s)=\int_0^\infty {\rm d}t\;{\rm e}^{-st}\;G_{\rm min/max}(z;t)$ $=s^{-1}[1-\hat{P}_{\rm fpt}(s;-1)]/[1-z^{\mp 1}\hat{P}_{\rm fpt}(s;-1)]$. Here, $\hat{P}_{\rm fpt}(s;x)={\rm e}^{Ax/2}\;{\rm e}^{-|x|\,\cosh^{-1}\left[s/2\nu+\cosh(A/2)\right]}-\delta_{x,0}$ is the Laplace transform of the first-passage-time probability density at site x. These expressions enable the computation of the Laplace transform of all the moments of the extrema from successive derivatives of the generating functions with respect to $\ln z$. In particular, the Laplace transform of the average minimum of entropy production reads $s\langle\hat{S}_{\rm min}(s)\rangle=-A/[\hat{P}_{\rm fpt}(s;-1)^{-1}-1]$. In the time domain, we may write this equality as $\langle S_{\rm min}(t)\rangle=-A\int_0^t{\rm d}T\sum_{x=1}^\infty P_{\rm fpt}(T;-x)$ [55] which can be written as (see appendix B):

$$\langle S_{\rm min}(t)\rangle=-\frac{A}{2\pi}\int_{-1}^{1}\frac{1-{\rm e}^{-2\nu t(\cosh(A/2)-y)}}{\left(\cosh(A/2)-y\right)^2}\sqrt{1-y^2}\;{\rm d}y. \tag{9}$$

Numerical simulations of the 1D biased random walk are in excellent agreement with equation (9) (figure 2, blue symbols). Note that equation (9) can also be expressed in terms of the Kampé de Fériet function F as $\langle S_{\rm min}(t)\rangle/A=-k_-t+{}^{2+0}F_{1+1}\left[\begin{matrix}[2\;1]\,,\,\varnothing\,,\,\varnothing\\ 3\,,\,2\,,\,2\end{matrix}\middle|-k_-t\;,\;-k_+t\right](k_-k_+t^2)/2$ (see appendix E). Interestingly, our simulations reveal (figure 2, red symbols) that the average maximum of entropy production minus the average entropy production at time t equals to minus the right-hand side of equation (9):

$$\langle S_{\rm max}(t)\rangle-\langle S(t)\rangle=-\langle S_{\rm min}(t)\rangle. \tag{10}$$

Equation (10) follows from the symmetry relation of the 1D biased random walk $\tilde{P}_{\rm fpt}(T;x)=P_{\rm fpt}(T;-x)$ and the relation $\langle S_{\rm max}(t)\rangle-\langle S(t)\rangle=A\int_0^t{\rm d}T\sum_{x=1}^\infty\tilde{P}_{\rm fpt}(T;x)$. Moreover, this symmetry extends to the distribution of minima and maxima of entropy production

$$P\left(S(0)-S_{\rm min}(t)=s\right)=P\left(S_{\rm max}(t)-S(t)=s\right), \tag{11}$$

where, in this case, $S(0)=0$. Figure 3 shows empirical distributions of entropy-production minima and maxima obtained from numerical simulations, which fulfil the symmetry relation (11).

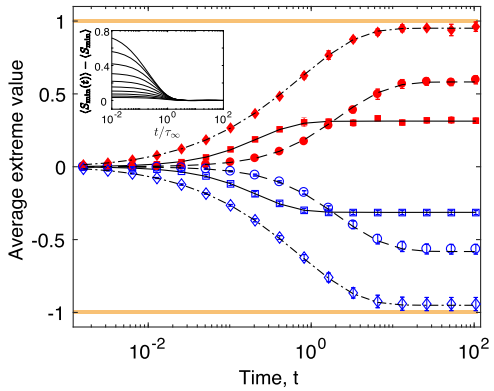

Figure 2. Average minimum $\langle S_{\min}(t)\rangle$ (blue open symbols) and average of the maximum minus the final value $\langle S_{\max}(t)\rangle - \langle S(t)\rangle$ (red filled symbols) of stochastic entropy production as a function of time of a 1D biased random walk. The symbols are averages over 10 sets of 10^3 numerical simulations; the error bars are the standard deviation of the mean values obtained from these sets. The black lines are obtained from numerical integration of equation (9) using the trapezoidal method. Simulation parameters: $A = 1$, $\nu = 0.5$ (squares); $A = 2$, $\nu = 2$ (circles); $A = 0.1$, $\nu = 100$ (diamonds). The horizontal orange lines at ± 1 correspond to the bound obtained using martingale theory [31]. Inset: $\langle S_{\min}(t)\rangle - \langle S_{\min}\rangle$ as a function of time rescaled by $\tau_\infty = [2\nu(\cosh(A/2) - 1)]^{-1}$. The different curves correspond to $\nu = 1$ and $0.5 \leqslant A \leqslant 5$.

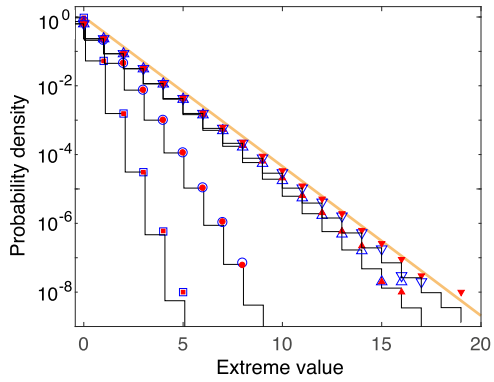

Figure 3. Empirical probability density of $-S_{\min}(t)$ (blue open symbols) and $S_{\max}(t) - S(t)$ (red filled symbols) obtained from 10^8 numerical simulations of a 1D biased random walk with parameters $A = 1$ and $\nu = 1$. Different symbols represent different integration times $t = 10^{-2}$ (squares), $t = 10^{-1}$ (circles), $t = 1$ (up triangles), $t = 10$ (down triangles). The black lines are the theoretical distributions for different values of t (from left to right) evaluated using equation (5). The orange line is an exponential distribution with mean value equal to minus one.

3. From a relaxation spectrum to a random-matrix approach

We now explore a connection between entropy-production extrema and random-matrix theory. More precisely, we relate the previously derived expressions for the average and distribution of extrema with eigenvalue distribution of specific random matrices. Equation (9) can also be written in terms of a finite relaxation spectrum (see appendix C)

$$\langle S_{\min}(t)\rangle = \langle S_{\min}\rangle \left(1 - \int_{\tau_0}^{\tau_\infty} \mathrm{e}^{-t/\tau}\, \rho(\tau/\bar{\tau})\frac{\mathrm{d}\tau}{\bar{\tau}}\right). \tag{12}$$

Here $\tau_0 \equiv \left(\sqrt{k_+} + \sqrt{k_-}\right)^{-2}$ is the minimal relaxation time of the extreme value statistics and $\tau_\infty \equiv \left(\sqrt{k_+} - \sqrt{k_-}\right)^{-2}$ is the maximal extrema relaxation time. Here ρ is the Marčenko–Pastur distribution, where times are normalized by $\bar{\tau} \equiv k_+/(k_+ - k_-)^2$. The Marčenko–Pastur distribution is given by [66]:

$$\rho(\lambda) \equiv \begin{cases} \dfrac{1}{2\pi\delta}\dfrac{\sqrt{(\lambda_+ - \lambda)(\lambda - \lambda_-)}}{\lambda} & \text{if } \lambda \in [\lambda_-, \lambda_+] \\ 0 & \text{if } \lambda \notin [\lambda_-, \lambda_+], \end{cases} \tag{13}$$

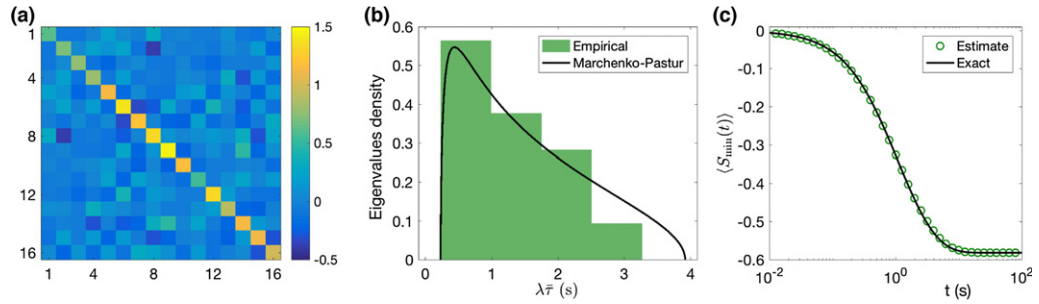

Figure 4. Illustration of the random-matrix approximation of the mean entropy production minimum. (a) Color-coded representation of a realization taken from the Wishart ensemble of real $m \times m$ random matrices with $m = 16$, $n = 44$ and $\beta = 1$. (b) Histogram of $\lambda\bar{\tau}$ (green bars), with λ denoting the eigenvalues of the random matrix shown in panel (a) and $\bar{\tau} = \mathrm{e}^{A/2}/(4\nu \sinh^2(A/2))$ a characteristic timescale. The corresponding Marcenko–Pastur distribution is shown as a solid line. (c) Average minimum $\langle S_{\min}(t)\rangle$ as a function of time (black solid line) shown together with the random-matrix approximation for the matrix shown in (a). In panels (b)–(c) we used the affinity $A = 1$ and rate $\nu = 1$, for which $n = \mathrm{e}^A \beta m \approx 43.5$.

with $\int_0^\infty \rho(\lambda)\mathrm{d}\lambda = 1$, where $\delta = k_-/k_+ = \mathrm{e}^{-A}$ and $\lambda_\pm = \left(1 \pm \sqrt{\delta}\right)^2 = (\sqrt{k_+} \pm \sqrt{k_-})^2/k_+$. Interestingly, the Marčenko–Pastur theorem states that $\rho(\lambda)$ is the distribution of eigenvalues in the large size limit of Hermitian matrices drawn from the ensemble of the Wishart–Laguerre random matrices [67–69], whose structure is explained below. Note that $\tau_0 = \lambda_-\bar{\tau}$ and $\tau_\infty = \lambda_+\bar{\tau}$. Because the distribution of $1/\lambda$ can also be expressed in terms of the Marčenko–Pastur distribution (see appendix C), equation (12) can be written in terms of Marčenko–Pastur distributed relaxation rates $k = \tau^{-1}$, see equation (C2). The average minimum given by equation (12) can be obtained from the generating function of the minimum distribution (see appendix C)

$$G_{\min}(z;t) = 1 + \frac{1-z}{\mathrm{e}^A - 1}\int_{\tau_0}^{\tau_\infty} \frac{1-\mathrm{e}^{-t/\tau}}{1+f(z)\tau}\rho(\tau/\bar{\tau})\frac{\mathrm{d}\tau}{\bar{\tau}}, \tag{14}$$

where $f(z) = k_+(z-1) + k_-(z^{-1}-1)$.

Equations (12)–(14) imply that the time at which the distribution of the extrema relaxes to its long time limit is given by the largest timescale of the relaxation spectrum $\tau_\infty = \bar{\tau}\lambda_+$. We illustrate this result in the inset of figure 2 which shows this for the case of $\langle S_{\min}(t)\rangle$. Furthermore, the Marčenko–Pastur theorem implies the following trace formula:

$$\langle S_{\min}(t)\rangle = \langle S_{\min}\rangle \left(1 - \lim_{m\to\infty}\frac{1}{m}\,\mathrm{Tr}\;\mathrm{e}^{-\mathbf{M}^{-1}t/\bar{\tau}}\right), \tag{15}$$

where $\mathbf{M}$ is an $m \times m$ random matrix drawn from the Wishart or Laguerre ensembles. It can be obtained as

$$\mathbf{M} = n^{-1}\mathbf{R}\mathbf{R}^{\mathrm{T}}. \tag{16}$$

Here, $\mathbf{R}$ is a random matrix and $\mathbf{R}^{\mathrm{T}}$ its transpose, $n = \mathrm{e}^A\beta m$ plays the role of a degree of freedom, with β the Dyson index of the Wishart or the Laguerre ensemble [70]. Hence, the rectangularity of $\mathbf{R}$ is linked to the bias of the random walk through $n/m = \beta\mathrm{e}^A$. In the case of real Wishart matrices for $A > 0$ the matrix $\mathbf{R}$ is an $m \times n$ rectangular random matrix, whose real entries are independent and identically distributed Gaussian random numbers with zero mean and unit variance. This implies that $\mathbf{M}$ is drawn from the distribution $P(\mathbf{M}) \sim (\det\mathbf{M})^{(n-m-1)/2}\,\mathrm{e}^{(n/2)\mathrm{Tr}\;\mathbf{M}}$. An alternative is the use of Laguerre matrices. The construction of these matrices and further details are given in appendix D.

Equation (15) can be approximated numerically using random matrices with finite but sufficiently large m. In practice, we use the following estimate:

$$\langle S_{\min}(t)\rangle \simeq \langle S_{\min}\rangle \left(1 - \frac{1}{m}\sum_{i=1}^{m}\mathrm{e}^{-t/(\bar{\tau}\lambda_i)}\right), \tag{17}$$

where λ_i is the ith eigenvalue of $\mathbf{M}$ drawn from either the Wishart or Laguerre random-matrix ensembles. This is illustrated in figure 4 using a 16×16 Wishart random matrix, shown in figure 4(a). This matrix has a set of eigenvalues λ with distribution shown as a histogram in figure 4(b) together with the Marcenko–Pastur distribution which is reached in the infinite matrix size limit. The corresponding extrema relaxation times correspond to values $\bar{\tau}\lambda$. The approximation for the relaxation of the mean minimum is given by equation (17) for $m = 16$ and shown together with the exact result in figure 4(c).

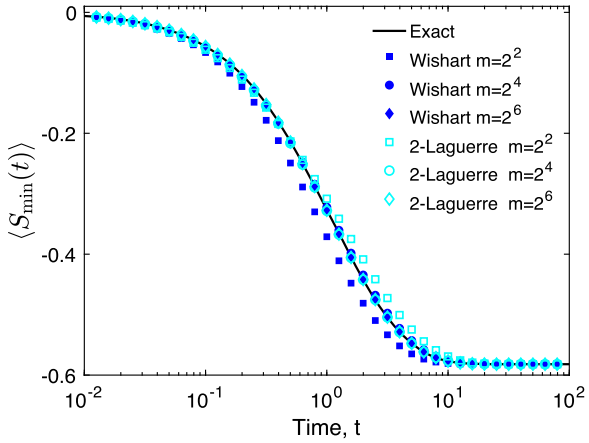

Figure 5. Finite-time average minimum of entropy production associated with 1D biased random walks as a function of time: exact result [equation (12), black line] and estimates obtained from the spectrum of *a single* $m \times m$ random matrix drawn from the Wishart (blue filled symbols) and the β-Laguerre ensembles ($\beta = 2$, open cyan symbols). The random-matrix estimates are obtained evaluating the right-hand side in equation (15), i.e. $\langle S_{\rm min}\rangle[1 - m^{-1}\sum_{i=1}^{m} e^{-t/(\bar{\tau}\lambda_i)}]$ with $\langle S_{\rm min}\rangle = -A/(e^A - 1)$, $\bar{\tau} \equiv k_+/(k_+ - k_-)^2 = e^{A/2}/(4\nu \sinh^2(A/2))$, and λ_i the ith eigenvalue of the corresponding Wishart/Laguerre random matrix. Values of the parameters: $A = \nu = 1$.

In figure 5 we show the approximation for different random-matrix ensembles of different sizes. We compute numerically the eigenvalues of a single random matrix of the Wishart ensemble and of a matrix drawn from the β-Laguerre ensemble with parameter $\beta = 2$. Notably, using a single 64×64 random matrix from the Wishart or Laguerre ensembles, we obtain an estimate of the average entropy production minimum that differs with respect to the exact value by at most 2% (at small times).

4. Extrema statistics of molecular motors

We now investigate whether similar results also hold for more complex stochastic models of molecular motors. We consider a biochemical process where a molecular motor's fluctuating motion is described by a continuous-time Markov jump process on a potential energy surface in two dimensions x and y (figure 6(a)). Here x denotes the spatial displacement of the motor along a discrete track of period ℓ, and y is a chemical reaction coordinate denoting the net number of fuel molecules spent by the motor.

The motion of the motor is biased along the track by a mechanical force $f_{\rm ext}$ applied to the motor. In addition, the motor hydrolyzes ATP with chemical potential difference $\Delta\mu$. We consider both $f_{\rm ext}$ and $\Delta\mu$ to be independent of the state of the motor, which corresponds to the limits where the external force and the concentration of fuel molecules are stationary. States (x, y) of the motor are in local equilibrium at temperature $T = \beta^{-1}$. The dynamics of the motor is as follows. From a given state the motor can perform, at a random time, a jump to eight adjacent states corresponding to the following four transitions and their reversals: (i) sliding along the track by a distance ℓ ($-\ell$) without consuming fuel but generating work in (against) the direction of the force, at a rate $k_{\rm m}^+$ ($k_{\rm m}^-$), with $k_{\rm m}^- = k_{\rm m}^+ \, e^{-\beta f_{\rm ext}\ell}$; (ii) consumption of one ATP (ADP) molecule without generating work, at a rate $k_{\rm c}^+$ ($k_{\rm c}^-$), with $k_{\rm c}^- = k_{\rm c}^+ \, e^{-\beta\Delta\mu}$; (iii) work generation in (against) the external force using ATP (ADP) at a rate $k_{\rm mc}^+$ ($k_{\rm mc}^-$), with $k_{\rm mc}^- = k_{\rm mc}^+ \, e^{-\beta(f_{\rm ext}\ell + \Delta\mu)}$ and (iv) work generation against (in) the external force using ATP (ADP) at a rate $k_{\rm cm}^+$ ($k_{\rm cm}^-$), with $k_{\rm cm}^- = k_{\rm cm}^+ \, e^{\beta(f_{\rm ext}\ell - \Delta\mu)}$. We use transition rates of the form $k_\alpha^\pm = \nu_\alpha \, e^{\pm A_\alpha/2}$, where ν_α give different weights to each transition type.

A single trajectory of the motor is a 2D random walk containing snapshots $(X(t), Y(t))$ of the state of the motor at time t. Here $X(t)$ is the spatial coordinate of the motor (with respect to its initial position) and $Y(t)$ is the reaction coordinate representing the net number of ATP molecules consumed up to time t. Note that when $Y(t)$ is negative, the motor has consumed more ADP than ATP molecules. The entropy production associated with a single trajectory of the molecular motor is $S(t) = A_{\rm m}X(t) + A_{\rm c}Y(t)$, where $A_{\rm m} = \beta f_{\rm ext}\ell$, $A_{\rm c} = \beta\Delta\mu$ are the mechanical and chemical affinities. Thus $S(t)$ is a random walk with four different step lengths $A_{\rm m}$, $A_{\rm c}$, $A_{\rm mc} \equiv A_{\rm m} + A_{\rm c}$ and $A_{\rm cm} \equiv -A_{\rm m} + A_{\rm c}$ corresponding to the jumps along the X, Y and the diagonal directions, respectively.

We perform numerical simulations of this 2D stochastic model of the molecular motor using Gillespie's algorithm, and evaluate the entropy flow associated with different trajectories of the motor. Obtaining exact extreme-value statistics in this model is challenging. However the following simple approximation provides good estimates. The average (figures 6(b) and 7(b)) of the entropy production extrema obtained from

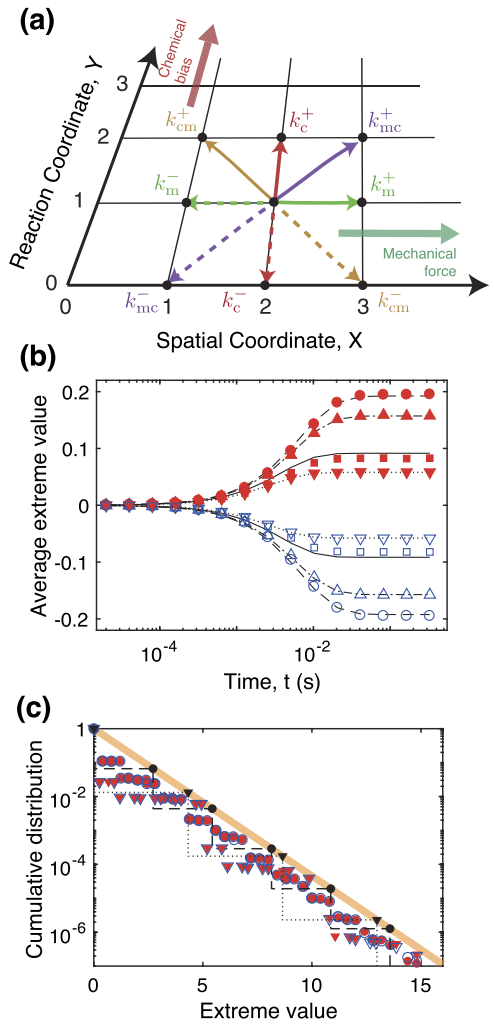

Figure 6. Entropy production extrema for a two-dimensional stochastic model of a molecular motor. (a) Sketch of the model with states given by the vertices of the 2D grid and the possible transitions from state (2, 1) marked with arrows. (b) Finite-time average minimum of entropy production ($\langle S_{\min}(t)\rangle$, blue open symbols) and average maximum of the entropy production minus its final value ($\langle S_{\max}(t) - S(t)\rangle$, red filled symbols) for values of the external force $f_{\text{ext}} = -2.5$ pN (squares, solid line), -1.5 pN (circles, dashed line), -0.5 pN (up triangles, dash-dot line), 0.5 pN (down triangles, dotted line). The lines are estimates obtained using equation (9) with effective parameters A_{eff} and ν_{eff} given by equations (18) and (19), see text for further details. (c) Cumulative distribution of $-S_{\min}(t)$ (blue open symbols) and of $S_{\max}(t) - S(t)$ (red filled symbols) for $f_{\text{ext}} = -1.5$ pN (circles) and 0.5 pN (down triangles), and $t = 50$ ms. The black symbols are estimates given by equation (3) with effective parameters A_{eff}, and the orange line is an exponential distribution with mean one. Values of the simulation parameters: $k_{\text{B}}T = 4.28$ pN nm, $\ell = 8$ nm, $\Delta\mu = 4k_{\text{B}}T$, $\nu_{\text{m}} = 10$ Hz, $\nu_{\text{c}} = 5$ Hz, $\nu_{\text{mc}} = 25$ Hz, and $\nu_{\text{cm}} = 1$ Hz. The numerical data were obtained from 10^8 simulations done using Gillespie's algorithm.

simulations can be approximated by equations (4)–(9) replacing A and ν by the effective parameters.

$$\nu_{\text{eff}} = \sum_{\alpha} \nu_{\alpha}, \tag{18}$$

$$A_{\text{eff}} = 2\cosh^{-1}\left(\sum_{\alpha} \frac{\nu_{\alpha}}{\nu_{\text{eff}}} \cosh\frac{A_{\alpha}}{2}\right), \tag{19}$$

where the index α runs over the four types of transitions $\alpha =$ m, c, mc and cm. This approximation based on effective parameters follows from considering effective 1D models with jumping rate $k^{+}_{\text{eff}} + k^{-}_{\text{eff}} = \sum_{\alpha} k^{+}_{\alpha} + k^{-}_{\alpha}$. Furthermore, we find for this model that the symmetry relations (10) and (11) between the distribution and the mean of finite-time minima and maxima of entropy production are satisfied with high accuracy in our numerical simulations, see figure 6. Notably, the distributions of entropy production maxima and minima coincide despite having irregular shapes for irrational ratios of the mechanical and chemical affinities.

The average extrema of the mechanical and chemical currents are shown in figure 7 as a function of the external force. The behaviour of these currents is known exactly from a mapping to 1D biased random

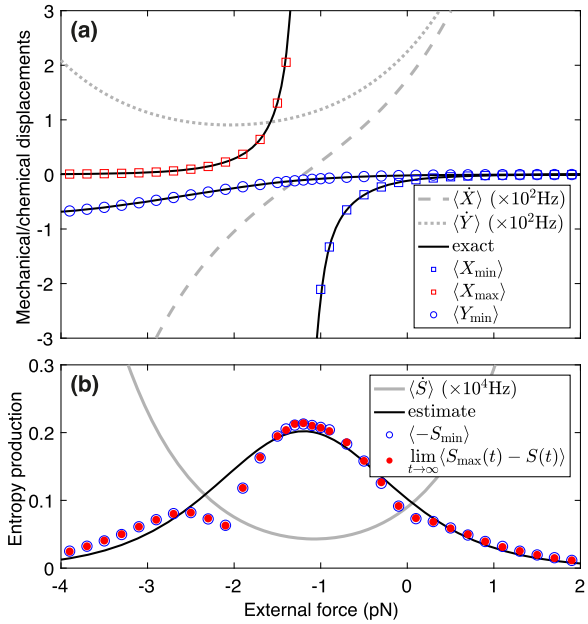

Figure 7. Numerical results of mechanical and chemical currents and of entropy production extrema as a function of the force for the two-dimensional stochastic model of a molecular motor of figure 6. (a) Average long time minima and maxima of mechanical steps $\langle X_{\rm min/max} \rangle$ (blue and red squares respectively) and average minima of chemical steps at long time $\langle Y_{\rm min} \rangle$ (blue circle) are shown as a function of the external force. The black lines are analytical results obtained using equation (4) with effective affinities $A_{x/y} = \ln(k^+_{x/y}/k^-_{x/y})$. For comparison, we also show the mechanical net stepping rates $k^+_x - k^-_x$ (dashed grey line) and the chemical net stepping rate $k^+_y - k^-_y$ (dotted grey line). $k^\pm_{x/y}$ are defined in equation (20). (b) Average long time minima (blue circles), maxima minus final value (red filled circles) and rate of total entropy production (grey line) as a function of the external force. The black line is an estimation obtained using equation (4) with the effective parameters $A_{\rm eff}$ and $\nu_{\rm eff}$ given by equations (18) and (19). The values of the fixed parameters are the same as in figure 6. The averages at long time in (a) and (b) were obtained at $t = 0.5$ s from 10^6 simulations done using Gillespie algorithm.

walks $X(t)$ and $Y(t)$ with effective forward and backward hopping rates given, respectively, by

$$k^\pm_x = k^\pm_{\rm m} + k^\pm_{\rm mc} + k^\mp_{\rm cm}, \qquad k^\pm_y = k^\pm_{\rm c} + k^\pm_{\rm mc} + k^\pm_{\rm cm}. \tag{20}$$

This yielding effective affinities $A_{x/y}$ and rates $\nu_{x/y}$ defined as in equation (2). This allows us to calculate the extreme value statistics of the net number of steps $X(t)$ and $Y(t)$, as illustrated in figure 7(a) as solid lines. Note that $A_x = \beta(f_{\rm ext} - f_{\rm stall})\ell$ is related to the mechanical affinity $A_{\rm m} = \beta f_{\rm ext}\ell$ and the stall force

$$f_{\rm stall} = \frac{1}{\beta\ell} \ln\left(\frac{1 + k^-_{\rm mc}/k^-_{\rm m} + k^+_{\rm cm}/k^-_{\rm m}}{1 + k^+_{\rm mc}/k^+_{\rm m} + k^-_{\rm cm}/k^+_{\rm m}} \right). \tag{21}$$

In the examples shown in figures 6 and 7, $f_{\rm stall} \simeq -1.2$ pN in the simulations. A_y and the chemical affinity $A_{\rm c}$ obey a similar relationship. We observe in figure 7(b) that the largest average extreme values of entropy production occur when the external force applied to the motor is near the stall force. Interestingly, the minima and maxima of the displacements, $X_{\rm min}$ and $X_{\rm max}$, show diverging averages when the stall force is approached from above or below respectively. Such behaviour could be measured in experiments on the statistics of the stepping of molecular motors near stall forces. Note that in figure 7 the long time limit of the average extrema is already reached at 0.1 s, see figure 6.

5. Discussion

We have derived analytical expressions for the distribution and moments of the finite-time minimum and maximum values of continuous-time biased random walks. Such stochastic processes provide minimal models to describe the fluctuating motion of molecular motors and cyclic enzymatic reactions that take place in a thermal reservoir and under non-equilibrium conditions induced by e.g. external forces and/or chemical reactions.

Our key results are: (i) exact statistics of the extrema of the position and the entropy production of a biased random walk; (ii) simple expressions at finite time in terms of an explicit relaxation-time spectrum; (iii) symmetry relations between distributions of extrema of stochastic entropy production; (iv) a novel

connection between extreme-value statistics of biased random walks and the Marčenko–Pastur distribution of random matrix theory.

For biased random walks, our results provide insights beyond the infimum law for nonequilibrium steady states, $\langle S_{\min}(t)\rangle \geqslant -1$, which states that the entropy production of a mesoscopic system plus its environment cannot be reduced on average by more than the Boltzmann constant. Further in continuous systems this bound is approached at large times, $\lim_{t\to\infty}\langle S_{\min}(t)\rangle = -1$. Here we have shown that the effects of discreteness are very important. At large times we find that a model dependent bound above -1 is reached, see equation (4) and figure 2. We find that for Markovian biased random walks with homogeneous stationary distribution, the difference between the minimum of entropy production and its initial value has the same statistics as the difference between its maximum and its final value, for any given time interval $[0, t]$, see equations (10) and (11). For random walks, such a 'min-max' symmetry has been noticed before [48]. This result further reveals that a supremum law for entropy production bounds the average of the difference between the maximum of entropy production and its value at a fixed time $t \geqslant 0$:

$$\langle S_{\max}(t)\rangle - \langle S(t)\rangle \leqslant 1. \tag{22}$$

The inequality (22) applies to any Markovian nonequilibrium stationary process. It can be obtained by applying the results of reference [31] to the process $R(t) = \mathcal{P}(X_{[0,t]})/\mathcal{P}(\tilde{X}_{[0,t]})$, exploiting the martingale property of $R(t)$. We have shown that the inequalities for the average extrema of entropy production and displacement of a biased random walk saturate in the limit of a small affinity $A \ll 1$. This limit corresponds to systems that exchange a small amount of heat with their environment—below the thermal energy $k_{\mathrm{B}}T$—in each forward or backward step of the walker. For larger values of A, our analytical expressions reveal that details on the discreteness in the walker's motion have a strong influence in the extrema statistics. The time-asymmetric parameter A fully determines the distribution of extrema at large times, as well as the shape of the relaxation time spectrum at finite times, whereas the time-symmetric rate constant ν (see equation (2)) only scales the time dependence.

Relaxation or retardation spectra describe the dynamics of systems governed by a continuum of characteristic times, such as those found in fractional rheology [71]. In this spirit, we expressed in equations (12) and (14) the extreme value statistics for a 1D biased continuous time random walk as a relaxation process, whose spectra of relaxation times follow the Marčenko–Pastur distribution (13).

A relation between statistical properties of stochastic processes and random matrices has also been found in different contexts [72–76]. In quantum-mechanical scattering problems, retardation rates have been described using spectra of Laguerre random matrices [74]. For classical Markovian relaxation processes, relaxation time spectra of the extreme value statistics have been discussed [53–55]. Path counting combinatorial problems have been shown to be described in terms of random matrix spectra [77]. These works suggest that large random matrices may be used as a combinatorial shortcut to tackle the relaxation of the statistics of extreme values.

Here we have shown that the finite-time extreme-value statistics of stochastic transport can be approximated by drawing suitable Wishart and Laguerre random matrices of finite size. The resulting random-matrix estimates can outperform the accuracy and convergence of Monte Carlo simulations that determine extrema statistics. As shown in figure 4, only a small number of eigenvalues are needed for an accurate description of the extreme value statistics.

The first passage times of non-Gaussian stochastic transport processes are well-described by a universal distribution involving their three first cumulants [64]. This distribution is similar to the distribution of first passage times given in equation (A19) that we obtain exactly. Note that the extreme value statistics of Gaussian transport such as a diffusion process is found as the small bias limit $A \ll 1$ of our 1D model (see (A7)). In particular, the velocity v and diffusion coefficient D for small bias are $v \simeq \nu A$ and $D \simeq \nu$. In this limit $A \to 0$, the characteristic relaxation time of extrema is $\bar{\tau} \simeq 1/(\nu A^2) \simeq D/v^2$ and the relaxation spectrum (13) reads:

$$\rho(\lambda) \simeq \begin{cases} \dfrac{1}{2\pi}\sqrt{\dfrac{4-\lambda}{\lambda}} & \text{if } \lambda \in [0,4] \\ 0 & \text{if } \lambda \notin [0,4]. \end{cases} \tag{23}$$

In other words, $\sqrt{\lambda}$ follows Wigner's semi-circle distribution [69]. From this result, we recover the finite-time average minimum of entropy production in the diffusive limit

$$\langle S_{\min}(t)\rangle \simeq \frac{1}{2\pi}\int_0^4 \left(\mathrm{e}^{-v^2\,t/\lambda D}-1\right)\sqrt{\frac{4-\lambda}{\lambda}}\,\mathrm{d}\lambda$$
$$= -\mathrm{erf}\left(\frac{\sqrt{s}}{2}\right)+\frac{s}{2}\,\mathrm{erfc}\left(\frac{\sqrt{s}}{2}\right)-\mathrm{e}^{-\frac{s}{4}}\sqrt{\frac{s}{\pi}}, \tag{24}$$

where $s = v^2 t/D$, cf. reference [31].

Our work has important consequences for the theory of nonequilibrium fluctuations of active molecular processes and biomolecules. For example, the statistics of the maximum excursion of a motor against its net motion along a track provides insights on the physical limits of pernicious effects of fluctuations at finite times, which can be relevant in e.g. the finite-time efficiency of enzymatic reactions responsible of polymerization processes, muscle contraction by molecular motors, etc. We have shown that the displacement of motors with small cycle affinity exhibits large extreme values on average. However, the associated extreme entropy flows are on average always bounded in absolute value by the Boltzmann constant; an improved bound can be estimated from our results for 1D biased random walks, as shown in our application to an homogeneous 2D biased random walks describing the motion of molecular motors. Insights of our theory could be also discussed in the context of more complex biomolecular stochastic processes (e.g. microtubule growth [7, 78] and transport in actin networks [79]). It will be interesting to extend our theory to Markovian and non-Markovian processes with time-dependent driving [80–85], stochastic processes with hidden degrees of freedom [86, 87], and also to explore whether extrema statistics from single-molecule experimental data reveal relaxation spectra described by the Marčenko–Pastur distribution.

Acknowledgments

We acknowledge enlightening discussions with Pierpaolo Vivo and fruitful discussion with Izaak Neri, Simone Pigolotti, Ken Sekimoto, and Carlos Mejía-Monasterio. AG acknowledges MPIPKS and ICTP for their hospitality, Bertrand Fourcade for his guidance towards MPIPKS, and EUR Light S & T for funding.

Appendix A. First-passage-times, large deviations, and absorption probabilities of biased random walks

In this section we review some knowledge of random walk theory (e.g. first-passage statistics [61]) to derive equation (6) in the main text i.e. the exact formula for the first-passage time distribution of a 1D continuous-time biased random walk. We also discuss large-deviation properties of this model, absorption probabilities using martingale theory.

A.1. Model and solution of the Master equation

We consider a continuous-time biased random walk in a discrete one-dimensional lattice, where $X(t) = \{0, \pm 1, \pm 2, \ldots\}$ denotes the position of the walker at time $t \geqslant 0$. We assume that $X(0) = 0$ and that the walker can jump from state $X(t) = x$ to $x + 1 (x - 1)$ at a rate $k_+ (k_-)$.

The waiting time at any site is exponentially distributed with the rate parameter $k_+ + k_-$. The probability $P_x(t) = P\,(X(t) = x)$ to find the walker at the lattice site x at time t obeys the master equation

$$\frac{\mathrm{d}P_x(t)}{\mathrm{d}t} = k_+ P_{x-1}(t) - (k_+ + k_-)P_x(t) + k_- P_{x+1}(t), \tag{A1}$$

with initial condition $P_x(0) = \delta_{x,0}$. From this evolution equation, a velocity $v = k_+ - k_-$ and a diffusion coefficient $D = (k_+ + k_-)/2$ can be defined. Its solution is the Skellam distribution [88] $P_{\mathrm{Sk}}(x; \mu_1, \mu_2) = (\mu_1/\mu_2)^{x/2} I_x(2\sqrt{\mu_1\mu_2})\mathrm{e}^{-(\mu_1+\mu_2)}$ with parameters $\mu_1 = k_+ t$ and $\mu_2 = k_- t$

$$P_x(t) = \left(\frac{k_+}{k_-}\right)^{x/2} I_x\left(2\sqrt{k_+ k_-}\,t\right)\mathrm{e}^{-(k_+ + k_-)t}, \tag{A2}$$

where $I_x(y)$ denotes the xth order modified Bessel function of the first kind. Equation (A2) follows from (A1) and the exact expression for the generating function of the modified Bessel function of the first kind $\sum_{x=-\infty}^{\infty} z^x I_x(y) = \mathrm{e}^{y(z+z^{-1})/2}$.

A.2. Large deviation and diffusion limit

We now discuss and review large deviation properties of the 1D biased random walk [89, 90] and relate them to the statistics of 1D drift diffusion process. For this purpose we consider the scaling limit of $P_x(t)$ given by equation (A2) for large $x \sim vt$, with $v = k_+ - k_-$ the net velocity of the walker. We assume a large deviation principle for $P_x(t)$ of the form

$$P_x(t) \sim \mathrm{e}^{-2\nu t J(x/vt)}. \tag{A3}$$

In order to derive an analytical expression for the rate function J, we first approximate the modified Bessel function in equation (A2) using a saddle point approximation

$$I_x(x/z) = \frac{1}{2\pi}\int_0^{2\pi} \mathrm{e}^{x(z^{-1}\cos\theta - \mathrm{i}\theta)}\,\mathrm{d}\theta \tag{A4}$$

$$\sim \frac{\mathrm{e}^{x(z^{-1}\cos\theta_0 - \mathrm{i}\theta_0)}}{\sqrt{2\pi x z^{-1}\cos\theta_0}} = \frac{\mathrm{e}^{x\left(\sqrt{1+z^{-2}} - \sinh^{-1} z\right)}}{\sqrt{2\pi x\sqrt{1+z^{-2}}}}, \tag{A5}$$

where the saddle point is given by $i\sin\theta_0 = z$ i.e. $i\theta_0 = \sinh^{-1}$ and we have used $\cos i\theta_0 = \cosh\theta_0$ and $z^{-1}\cosh\sinh^{-1} z = \sqrt{1+z^{-2}}$. The rate function $J(u)$ with $u = x/vt$ can be evaluated from the leading term of equation (A2) which is found using equation (A5):

$$\begin{aligned} J(u) &= J\left(z/\sinh(A/2)\right) \\ &\equiv \lim_{t\to\infty} -\frac{\ln P_{2\nu t z}(t)}{2\nu t} \\ &= \lim_{t\to\infty} \frac{2\cosh(A/2)\nu t - \nu t z A - \ln I_{2\nu t z}(2\nu t)}{2\nu t} \\ &= \cosh\frac{A}{2} + z\left(\sinh^{-1} - \frac{A}{2}\right) - \sqrt{1+z^2}, \end{aligned} \tag{A6}$$

where $z = u\sinh(A/2) = x/2\nu t$ and the change of variables $(k_+, k_-) \to (A, \nu)$ have been used for convenience.

In the vicinity of the minimum where $u \sim 1$ and thus $z \sim \sinh(A/2)$, the large deviation function behaves as

$$J(u) = \frac{\sinh(A/2)^2(u-1)^2}{2\cosh(A/2)} + \frac{\sinh(A/2)^4(u-1)^3}{6\cosh(A/2)^3} + O(u-1)^4. \tag{A7}$$

Interestingly, the ratio between the second and the leading term of (A7), given by $\tanh(A/2)^2(u-1)/3$, vanishes for small deviations $u \sim 1$ but also for large deviations in the limit of a small bias $A \ll 1$. The continuum limit of the biased random walk for A small simplifies to the drifted Brownian motion $P_x(t) = \mathrm{e}^{-(x-vt)^2/4Dt}/\sqrt{4\pi Dt}$, where the polynomial prefactor is recovered by normalization, and we have used the expressions for the velocity $v = 2\nu\sinh(A/2)$ and the diffusion coefficient $D = \nu\cosh(A/2)$. In this regard, the 1D biased random walk can be seen as a generalization of the drifted Brownian motion for any bias. A finite bias modifies occurrences of extreme large deviations with respect to those occurring in the drift diffusion process. Consequently, the bias A is expected to affect the extreme value statistics of the process, as shown below.

A.3. Martingales and absorption probabilities

In this subsection we employ martingale theory to derive an analytical expression of the absorption probability $P_{\mathrm{abs}}(-x)$ for a 1D biased random walk starting at $x = 0$ to ever reach an absorbing boundary located at $-x < 0$.

We first show explicitly that $\mathrm{e}^{-S(t)}$ is a martingale process with respect to $X(t)$, i.e.

$$\langle \mathrm{e}^{-S(t)} | X_{[0,t']}\rangle = \mathrm{e}^{-S(t')}, \tag{A8}$$

for $t \geqslant t'$. In words, the average of $\mathrm{e}^{-S(t)}$ over all trajectories with common history $X_{[0,t']}$ up to time $t' \leqslant t$ equals to its value at the last time of the conditioning $\mathrm{e}^{-S(t')}$. The proof is as follows:

$$\begin{aligned} \langle \mathrm{e}^{-S(t)} | X_{[0,t']}\rangle &= \langle \mathrm{e}^{-[S(t)-S(t')]} | X_{[0,t']}\rangle \mathrm{e}^{-S(t')} \\ &= \langle \mathrm{e}^{-S(t-t')}\rangle\ \mathrm{e}^{-S(t')} \end{aligned}$$

$$= \mathrm{e}^{-S(t')} \sum_{x=-\infty}^{\infty} P_x(\Delta t) \left(\frac{k_-}{k_+}\right)^x$$

$$= \mathrm{e}^{-S(t')}\ \mathrm{e}^{-(k_+ + k_-)\Delta t} \underbrace{\sum_{x=-\infty}^{\infty} \left(\frac{k_+}{k_-}\right)^{-x/2} I_x\left(2\sqrt{k_+ k_-}\,\Delta t\right)}_{=\mathrm{e}^{(k_+ + k_-)\Delta t}}$$

$$= \mathrm{e}^{-S(t')}. \tag{A9}$$

□

In the first and second lines we have used the additive property and the Markov property of entropy production, respectively. In the third line we have used the definitions $\Delta t \equiv t - t'$ and $S(t) = X(t)\ln(k_+/k_-)$. In the fourth line we have used the identity $\sum_{x=-\infty}^{\infty} z^x I_x(y) = \mathrm{e}^{y(z+z^{-1})/2}$.

We remark that the proof sketched above can be simplified using the integral fluctuation relation $\langle e^{-S(t-t')}\rangle = 1$ in the second line, which holds for any $t \geqslant t'$ [91, 92]. It has been shown [31, 93] that the martingality of $\mathrm{e}^{-S(t)}$ implies a set of integral fluctuation relations at stopping times

$$\langle \mathrm{e}^{-S(T)}\rangle = 1, \tag{A10}$$

where T is any bounded stopping time, i.e. a stochastic time at which the process $X(t)$ satisfies for the first time a certain criterion. In particular, equation (A10) holds for the first-passage time T_2 of $X(t)$ to reach any of two absorbing barriers located at $-x_-$ and x_+, with x_+ and x_- two arbitrary positive integer numbers. When applying equation (A10) to this particular stopping time, we can unfold the average in the left-hand side using the absorption probabilities

$$\begin{aligned}\langle \mathrm{e}^{-S(T_2)}\rangle &= P_{\mathrm{abs}}(x_+)\langle \mathrm{e}^{-S(T_2)}\rangle_+ + P_{\mathrm{abs}}(x_-)\langle \mathrm{e}^{-S(T_2)}\rangle_- \\ &= P_{\mathrm{abs}}(x_+)\mathrm{e}^{-Ax_+} + P_{\mathrm{abs}}(x_-)\mathrm{e}^{Ax_-} \\ &= \mathrm{e}^{-Ax_+} + P_{\mathrm{abs}}(x_-)[\mathrm{e}^{Ax_-} - \mathrm{e}^{-Ax_+}] \\ &= 1,\end{aligned} \tag{A11}$$

where in the second line we have used the fact that $\mathrm{e}^{-S(T_2)} = \mathrm{e}^{-Ax_+}$ with probability $P_{\mathrm{abs}}(x_+)$ and $\mathrm{e}^{-S(T_2)} = \mathrm{e}^{Ax_-}$ with probability $P_{\mathrm{abs}}(x_-)$. In the third line we have used $P_{\mathrm{abs}}(x_+) + P_{\mathrm{abs}}(x_-) = 1$, and in the fourth line equation (A10). Solving the third line equation (A11) for the absorption probability we obtain

$$P_{\mathrm{abs}}(x_-) = \frac{1 - \mathrm{e}^{-Ax_+}}{\mathrm{e}^{Ax_-} - \mathrm{e}^{-Ax_+}}. \tag{A12}$$

Taking the limit $x_+ \to \infty$ in equation (A12) we obtain the well-known analytical expression for the absorption probability

$$P_{\mathrm{abs}}(x) = \mathrm{e}^{-Ax}, \tag{A13}$$

which we used to derive the analytical expressions − equations (3) and (4) − of the distribution and mean of the global minimum of entropy production in the biased random walk.

A.4. First-passage-time distribution

The first-passage-time density $P_{\mathrm{fpt}}(t'; x)$ can be derived from the solution of the Master equation (A1) with an absorbing boundary at site $x \neq 0$, with x an integer number [61]. It can also be derived from the distribution of the walker using Laplace transforms through the renewal equation:

$$P_x(t) = \int_0^t P_{\mathrm{fpt}}(t'; x) P_0(t - t')\mathrm{d}t'. \tag{A14}$$

where $P_0(t)$ is the probability to be at a state at time t when the system was at the same state at $t = 0$. This convolution integral becomes a product in the Laplace domain, for any $x \neq 0$:

$$\hat{P}_x(s) = \hat{P}_0(s)\hat{P}_{\mathrm{fpt}}(s; x) = \frac{\mathrm{e}^{Ax/2}\left(h(s) + \sqrt{h(s)^2 - 1}\right)^{-x}}{2\nu\sqrt{h(s)^2 - 1}}, \tag{A15}$$

where

$$h(s) \equiv \frac{s + k_+ + k_-}{2\sqrt{k_+ k_-}} = \frac{s}{2\nu} + \cosh(A/2), \tag{A16}$$

and

$$\hat{P}_0(s) = \int_0^\infty \mathrm{d}t\ \mathrm{e}^{-st} P_0(t) = \frac{1}{2\nu\sqrt{h^2(s)-1}}. \tag{A17}$$

We thus obtain, using equations (A16) and (A17) in (A15)

$$\begin{aligned}\hat{P}_{\mathrm{fpt}}(s;x) &= \mathrm{e}^{Ax/2}\left(h(s)+\sqrt{h(s)^2-1}\right)^{-x} \\ &= \mathrm{e}^{Ax/2-|x|\cosh^{-1}\left(s/2\nu+\cosh(A/2)\right)}.\end{aligned} \tag{A18}$$

In the above equations and in the following we will use the variables $\nu = (k_+k_-)^{1/2}$ and $A = \ln(k_+/k_-)$, see equation (2) in the main text. The inverse Laplace transform of equation (A18) implies $P_{\mathrm{fpt}}(t;x) = (|x|/t)P_x(t)$:

$$P_{\mathrm{fpt}}(t;x) = \frac{|x|}{t}\ \mathrm{e}^{Ax/2} I_x(2\nu t)\mathrm{e}^{-2\ \cosh(A/2)\nu t}, \tag{A19}$$

which is equation (6) in the main text.

Appendix B. Exact extrema statistics for the 1D biased random walk

In this section, we use generating functions to derive the statistics of the finite-time extrema of entropy production. In particular, we focus on the generating function for the probability $G_{\min}$ of the minimum and the generating function for the absorption probability G_{abs}, which are defined respectively as

$$G_{\min}(z;t) \equiv \sum_{x=0}^{\infty} z^{-x}\, P\left(S_{\min}(t) = -Ax\right), \tag{B1}$$

$$G_{\mathrm{abs}}(z;t) \equiv \sum_{x=1}^{\infty} z^{-x} P_{\mathrm{abs}}(-x;t). \tag{B2}$$

These two generating functions are related by

$$G_{\min}(z;t) = 1 + G_{\mathrm{abs}}(z;t)(1-z). \tag{B3}$$

Moments and probabilities follow taking derivatives of the generating functions (B1) with respect to z

$$\left\langle S_{\min}(t)^m \right\rangle = \left.\frac{\partial^m G_{\min}(z^A;t)}{\partial(\ln z)^m}\right|_{z=1}, \tag{B4}$$

$$P\left(S_{\min}(t) = -mA\right) = \left.\frac{\partial^m G_{\min}(z;t)}{m!\,\partial(z^{-1})^m}\right|_{z^{-1}=0}. \tag{B5}$$

For instance, inserting (B3) into (B4) to compute the first moment reduces to the simple expression

$$\left\langle S_{\min}(t)\right\rangle = -AG_{\mathrm{abs}}(1;t). \tag{B6}$$

B.1. Finite time statistics in the Laplace domain

We rewrite the probability-generating function $G_{\min}$ using the first-passage-time density derived above (A18). First we use the fact the first-passage-time density is the derivative of the absorption probability, $\hat{P}_{\mathrm{fpt}}(s;x) = s\hat{P}_{\mathrm{abs}}(x;s) - \delta_{x,0}$, which holds for any x. Equation (A19) implies that the Laplace transform $\hat{P}_{\mathrm{fpt}}(s;-x)$ of the first-passage-time probability to reach an absorbing site located at $-x$, with $x \geqslant 1$, can be expressed as the xth power of the Laplace transform $\hat{P}_{\mathrm{fpt}}(s;-1)$ of the first-passage time probability to reach $x = -1$:

$$\hat{P}_{\mathrm{fpt}}(s;-x) = \hat{P}_{\mathrm{fpt}}(s;-1)^x. \tag{B7}$$

Consequently, the statistics of the minimum (maximum) can be expressed in terms of just $\hat{P}_{\mathrm{fpt}}(s;-1)$ ($\hat{P}_{\mathrm{fpt}}(s;1)$). Using equations (B1)–(B3) and (B7), we derive the generating functions in terms of $\hat{P}_{\mathrm{fpt}}(s;-1)$

$$s\hat{G}_{\mathrm{abs}}(z;s) = \sum_{x=1}^{\infty} z^{-x}\hat{P}_{\mathrm{fpt}}(s;-1)^x = \frac{z^{-1}\hat{P}_{\mathrm{fpt}}(s;-1)}{1-z^{-1}\hat{P}_{\mathrm{fpt}}(s;-1)}, \tag{B8}$$

$$s\hat{G}_{\min}(z;s) = \frac{1-\hat{P}_{\mathrm{fpt}}(s;-1)}{1-z^{-1}\hat{P}_{\mathrm{fpt}}(s;-1)}. \tag{B9}$$

Because $\hat{P}_{\rm fpt}(s;-1)=\mathrm{e}^{-A/2}(h(s)+\sqrt{h(s)^2-1})$ is algebraic, all the moments and probabilities, obtained from equations (B4) and (B5), are algebraic expressions. For instance, the Laplace transform of the mean minimum is obtained directly from (B6) and (B8):

$$s\langle\hat{S}_{\rm min}\ (s)\rangle=\frac{-A}{\hat{P}_{\rm fpt}(s;-1)^{-1}-1}. \tag{B10}$$

B.2. Integral representations of extreme value statistics

We start from the first-passage-time density formula (A19) and we exploit two properties of the modified Bessel function of the first kind. This allows us to rewrite the absorption probability as a definite integral of trigonometric and hyperbolic functions and the parameters A and ν:

$$\begin{aligned}P_{\rm abs}(x;t)&=\int_0^t P_{\rm fpt}(t';x)\mathrm{d}t'\\&=\mathrm{e}^{Ax/2}\int_0^t\frac{|x|}{t'}I_x(2\nu t')\mathrm{e}^{-2\ \cosh(A/2)\nu t'}\ \mathrm{d}t'\end{aligned} \tag{B11}$$

$$=\mathrm{e}^{Ax/2}\int_0^\pi\int_0^t\mathrm{e}^{-2\nu t'(\cosh(A/2)-\cos\ \theta)}2\nu\ \mathrm{d}t'\left(\cos\left[(|x|-1)\theta\right]-\cos\left[(|x|+1)\theta\right]\right)\frac{\mathrm{d}\theta}{2\pi} \tag{B12}$$

$$=\mathrm{e}^{Ax/2}\int_0^\pi\frac{1-\mathrm{e}^{-2\nu t(\cosh(A/2)-\cos\ \theta)}}{\cosh(A/2)-\cos\ \theta}\left(\cos\left[(|x|-1)\theta\right]-\cos\left[(|x|+1)\theta\right]\right)\frac{\mathrm{d}\theta}{2\pi}. \tag{B13}$$

In (B11) we have used equation (A19). In (B12) we have used the definition $I_x(y)=(1/\pi)\int_0^\pi \mathrm{e}^{y\ \cos\ \theta}\ \cos(x\theta)\mathrm{d}\theta$ and the property $I_x(y)=(y/2x)[I_{x-1}(y)-I_{x+1}(y)]$. Finally in (B13) we have performed the integration over t. Using equation (B13), we express the generating function of the absorption probability as an integral:

$$\begin{aligned}G_{\rm abs}(z;t)&=\sum_{x=1}^\infty z^{-x}P_{\rm abs}(-x;t)\\&=\int_0^\pi\frac{1-\mathrm{e}^{-2\nu t(\cosh(A/2)-\cos\ \theta)}}{\cosh(A/2)-\cos\ \theta}\frac{(\sin\ \theta)^2}{\cosh(A/2+\ln\ z)-\cos\ \theta}\ \frac{\mathrm{d}\theta}{2\pi},\end{aligned} \tag{B14}$$

Where we have used in the above equation the identity

$$\sum_{x=1}^\infty\mathrm{e}^{-\alpha x}\left(\cos\left((x-1)\theta\right)-\cos\left((x+1)\theta\right)\right)=\frac{(\sin\ \theta)^2}{\cosh\alpha-\cos\theta}, \tag{B15}$$

which follows from the generating function of Chebyshev polynomials of the first kind $T_x(\cos\theta)\equiv\cos(x\theta)$. Performing the change of variable $y=\cos\theta$ in equation (B14), and setting $z=1$ (we recall $\langle S_{\rm min}(t)\rangle=-AG_{\rm abs}(1,t)$, see equation (B6)) we obtain equation (9) in the main text:

$$\langle S_{\rm min}(t)\rangle=-\frac{A}{2\pi}\int_{-1}^1\frac{1-\mathrm{e}^{-2\nu t\left(\cosh(A/2)-y\right)}}{\left(\cosh(A/2)-y\right)^2}\sqrt{1-y^2}\ \mathrm{d}y. \tag{B16}$$

□

Appendix C. Extrema statistics and Marčenko–Pastur distribution

In this section, we derive analytical expressions for the extrema statistics of 1D biased random walks in terms of the Marčenko–Pastur distribution (13) of random matrix theory, copied here for convenience:

$$\rho(\lambda)\equiv\begin{cases}\dfrac{1}{2\pi\delta}\dfrac{\sqrt{(\lambda_+-\lambda)(\lambda-\lambda_-)}}{\lambda} & \text{if}\ \ \lambda\in[\lambda_-,\lambda_+]\\ 0 & \text{if}\ \ \lambda\notin[\lambda_-,\lambda_+],\end{cases} \tag{C1}$$

where λ is a positive random variable, $\delta\leqslant 1$ a parameter, and $\lambda_\pm=\left(1\pm\sqrt{\delta}\right)^2$. Note that this distribution is normalized with mean $\int_{\lambda_-}^{\lambda_+}\lambda\rho(\lambda)\mathrm{d}\lambda=1$.

C.1. Average value of the finite-time minimum of entropy production

Performing the changes of variable $k = 2\nu(\cosh(A/2) - y)$, as well as $\tau = 1/k$, in equation (B16) we obtain

$$\langle S_{\min}(t)\rangle = -\frac{A}{2\pi}\int_{k_0}^{k_\infty} \frac{1-\mathrm{e}^{-kt}}{k}\sqrt{(k_\infty - k)(k-k_0)}\,\frac{\mathrm{d}k}{k} \tag{C2}$$

$$= -\frac{A}{2\pi}\int_{\tau_0}^{\tau_\infty} \left(1-\mathrm{e}^{-t/\tau}\right)\sqrt{\frac{(\tau_\infty - \tau)(\tau-\tau_0)}{\tau_\infty\tau_0}}\,\frac{\mathrm{d}\tau}{\tau}, \tag{C3}$$

where we have introduced the variables

$$k_{\infty/0} \equiv (\sqrt{k_+} \pm \sqrt{k_-})^2, \tag{C4}$$

$$\tau_{\infty/0} \equiv \frac{1}{k_{0/\infty}}. \tag{C5}$$

Thus, the average entropy production minimum can be expressed as exponential relaxation process with a spectrum of relaxation times distributed according to Marčenko–Pastur distributions (C1)

$$\langle S_{\min}(t)\rangle = -Ak_-\int_{k_0}^{k_\infty} \frac{1-\mathrm{e}^{-kt}}{k}\rho(k/\bar{k})\frac{\mathrm{d}k}{\bar{k}} \tag{C6}$$

$$= \langle S_{\min}\rangle \int_{\tau_0}^{\tau_\infty} (1-\mathrm{e}^{-t/\tau})\rho(\tau/\bar{\tau})\frac{\mathrm{d}\tau}{\bar{\tau}}, \tag{C7}$$

where

$$\bar{k} \equiv k_+, \tag{C8}$$

$$\bar{\tau} \equiv \frac{k_+}{(k_+ - k_-)^2} = \frac{\sqrt{\tau_0\tau_\infty}}{1-\mathrm{e}^{-A}}, \tag{C9}$$

and

$$\delta = \frac{k_-}{k_+} = \mathrm{e}^{-A}. \tag{C10}$$

Note that equation (C7) provides equation (12) of the main text.

C.2. Generating functions of the absorption probability and the minimum

The generating function for the absorption probability can also be expressed using Marčenko–Pastur distributions. Using the same method as described above for equation (B14), we find

$$G_{\mathrm{abs}}(z;t) = k_-\int_{k_0}^{k_\infty} \frac{1-\mathrm{e}^{-kt}}{k+f(z)}\rho(k/\bar{k})\mathrm{d}k/\bar{k} \tag{C11}$$

$$= \frac{1}{\mathrm{e}^A - 1}\int_{\tau_0}^{\tau_\infty} \frac{1-\mathrm{e}^{-t/\tau}}{1+f(z)\tau}\rho(\tau/\bar{\tau})\mathrm{d}\tau/\bar{\tau}, \tag{C12}$$

where

$$f(z) \equiv k_+(z-1) + k_-(z^{-1}-1). \tag{C13}$$

Using equations (C12) and (B3) we obtain the generating function of the distribution of minima given by equation (14) in the main text

$$G_{\min}(z;t) = \frac{1}{\mathrm{e}^A - 1}\int_{\tau_0}^{\tau_\infty} \frac{1-\mathrm{e}^{-t/\tau}}{1+f(z)\tau}\rho(\tau/\bar{\tau})\mathrm{d}\tau/\bar{\tau}. \tag{C14}$$

C.3. Laplace transforms

Taking the Laplace transform of equation (C11), we obtain

$$s\hat{G}_{\mathrm{abs}}(z;s) = k_-\int_{k_0}^{k_\infty} \frac{k}{k+s}\frac{\rho(k/\bar{k})}{k+f(z)}\,\frac{\mathrm{d}k}{\bar{k}}. \tag{C15}$$

Equation (C15) and (B6) imply that the Laplace transform of the average minimum can be written as a Stieltjes-like transform of the Marčenko–Pastur distribution for the variable k

$$s\langle \hat{S}_{\min}(s)\rangle = -Ak_- \int_{k_0}^{k_\infty} \frac{\rho(k/\bar{k})}{k+s}\,\frac{\mathrm{d}k}{\bar{k}}, \tag{C16}$$

and similar relations hold for moments of any order. Notably, equations (C15) and (C16) have a similar mathematical structure as the Laplace transform of the first-passage-time density of Markovian stochastic processes found in [55], where instead $\hat{P}_{\mathrm{fpt}}(s;x)$ is expressed as a weighted discrete sum of relaxation modes.

Appendix D. Random-matrix estimates of extreme-value statistics

In this section we discuss the connection between the relaxation spectrum of first-passage and extrema statistics in the 1D biased random walk with random-matrix theory. We now describe how one can estimate finite-time statistics of the minimum entropy production from the spectrum of suitable random matrices. For this purpose, we use a celebrated result by Marčenko and Pastur [66]. Consider a real $m \times m$ Wishart matrix defined as

$$\mathbf{W} = \frac{1}{n}\mathbf{R}\mathbf{R}^{\mathrm{T}}, \tag{D1}$$

where $\mathbf{R}$ (its transpose $\mathbf{R}^{\mathrm{T}}$) is an $m \times n$ random matrix, with $n \geqslant m$. The random matrix $\mathbf{R}$ is filled with independent identically distributed (i.i.d.) random variables drawn from a normal distribution of zero mean and unit variance, i.e. $\mathbf{R}_{ij} \sim \mathcal{N}(0,1)$, for all $i,j \leqslant m$. The resulting positive definite random matrix follows the Wishart distribution of degree of freedom n and density $c_{n,m}(\det \mathbf{w})^{(n-m-1)/2}\mathrm{e}^{\mathrm{Tr}\mathbf{w}\ n/2}$ (where $c_{n,m}$ is a normalization factor). Following Marčenko and Pastur, the eigenvalues λ of the Wishart random matrix $\mathbf{W}$ are asymptotically distributed according to the distribution (C1) in the limit $n,m \to \infty$ with finite *rectangularity* $m/n \to \delta < 1$. It has been shown that this asymptotic result also holds when all $\mathbf{R}_{ij}$ are i.i.d. random variables drawn from any distribution of zero mean and unit variance [69].

We now put in practice Marčenko and Pastur's result, namely we find random matrices whose spectral density matches with that of the relaxation spectrum of the average minimum of entropy production. This can be achieved e.g. by using a Wishart random matrix of rectangularity m/n identified as $\delta = k_-/k_+ = \mathrm{e}^{-A}$ in terms of the bias A of the walker, i.e. we draw a real $m \times n$ Wishart random matrix $\mathbf{W}$ with $m,n \gg 1$ and $m/n \simeq \mathrm{e}^{-A}$ (for instance $n = \lceil \mathrm{e}^{A} m \rceil$). Then we evaluate the m eigenvalues λ_i of the matrix $\mathbf{W}$ and we give them a dimension using equations (C8) and (C9) and performing the changes of variables $k = \lambda\bar{k}$ in equation (C6) and $\tau = \lambda\bar{\tau}$ in equation (C7) respectively. We thus obtain the following two estimates, $\langle \tilde{S}_{\min}(t)\rangle_k$ and $\langle \tilde{S}_{\min}(t)\rangle_\tau$, for the average entropy production minimum:

$$\langle \tilde{S}_{\min}(t)\rangle_k \equiv -A\ \mathrm{e}^{-A}\ \frac{1}{m}\sum_{i=1}^{m} \frac{1-\mathrm{e}^{-\lambda_i \bar{k} t}}{\lambda_i}, \tag{D2}$$

$$\langle \tilde{S}_{\min}(t)\rangle_\tau \equiv \langle S_{\min}\rangle\ \frac{1}{m}\sum_{i=1}^{m} \left(1-\mathrm{e}^{-t/\lambda_i \bar{\tau}}\right), \tag{D3}$$

where $\bar{k} = k_+$ and $\bar{\tau} = k_+/(k_+ - k_-)^2$ as identified previously. These estimates converge respectively to the exact result in the limit of a large matrix size. Using equations (C11) and (C12), the same procedure can be applied to estimate the generating function and any order moment of the distribution of entropy production extrema.

To test the convergence of these estimates, we define their relative error $\epsilon_k(t)$ and $\epsilon_\tau(t)$ as the relative difference

$$\epsilon_{k,\tau}(t) \equiv \frac{\langle \tilde{S}_{\min}(t)\rangle_{k,\tau} - \langle S_{\min}(t)\rangle}{\langle S_{\min}(t)\rangle}, \tag{D4}$$

which is a random real quantity for both k and τ estimates. Their limiting values are related and can be calculated analytically:

$$\epsilon_{\min} \equiv \lim_{t\to 0} \epsilon_k(t) = \lim_{t\to\infty} \epsilon_\tau(t) = 0 \tag{D5}$$

$$\begin{aligned}\epsilon_{\max} &\equiv \lim_{t\to\infty} \epsilon_k(t) = \lim_{t\to 0} \epsilon_\tau(t) \\ &= (1-\mathrm{e}^{-A})\left(\frac{1}{m}\sum_{i=1}^{m}\frac{1}{\lambda_i}\right) - 1,\end{aligned} \tag{D6}$$

which vanishes in the limit of a large random matrix because $\langle 1/\lambda\rangle_\rho = 1/(1-\mathrm{e}^{-A})$, with $\langle \ldots\rangle_\rho$ denoting an average over the Marčenko–Pastur distribution (C1). From the limits (D5), we conclude that the

estimate (D2) is advantageous to study the short-time behaviour whereas (D3) is most suited for large-time asymptotics. Our numerical results show that $|\epsilon_k(t)| \leqslant |\epsilon_{\max}|$ and also $|\epsilon_\tau(t)| \leqslant |\epsilon_{\max}|$ for all tested parameter values and for all times t. Therefore we will use $\epsilon_{\max}$ given by equation (D6) as a conservative bound for the relative error of the random-matrix estimates at any time t.

The estimates introduced above rely on the fact that one can achieve a rectangularity $m/n \simeq \mathrm{e}^{-A}$ with large enough random matrices. Because e^{-A} is not a rational number in general, it is desirable to develop random-matrix estimates that achieve the Marčenko–Pastur distribution accurately for any value of A. Following [67], the β-Laguerre matrices are an alternative ensemble whose spectral density tends asymptotically to the distribution MP(e^{-A}) in the large size limit. A β-Laguerre $m \times m$ random matrix $\mathbf{L}$ is defined as

$$\mathbf{L} = \frac{1}{n}\mathbf{R}\mathbf{R}^{\mathrm{T}}, \tag{D7}$$

where $n = m\beta\mathrm{e}^{A}$, with β the Dyson index of the ensemble. Here, $\mathbf{R}$ is an $m \times m$ random matrix with all entries equal to zero except the $m \times (m-1)$ diagonal and sub-diagonal elements. The non-zero entries R_{ij} are drawn following $\chi(d_{ij})$ distributions of d_{ij} degrees of freedom:

$$\mathbf{R} = \begin{bmatrix} R_{1,1} & & & \\ R_{2,1} & R_{2,2} & & \\ & R_{3,2} & R_{3,3} & \\ & & \ddots & \ddots \end{bmatrix} \sim \begin{bmatrix} \chi(d_{1,1}) & & & \\ \chi(d_{2,1}) & \chi(d_{2,2}) & & \\ & \chi(d_{3,2}) & \chi(d_{3,3}) & \\ & & \ddots & \ddots \end{bmatrix}. \tag{D8}$$

The random variable $Z_{ij} = \sqrt{\sum_{k=1}^{d_{ij}} X_k^2}$, where the $X_k \sim \mathcal{N}(0,1)$ are i.i.d., follows the $\chi(d_{ij})$ distribution. Equivalently, one can obtain a random variable that follows the $\chi(d_{ij})$ distribution by taking the square root of a random variable drawn from a chi-square distribution $\chi^2(d_{ij})$. The degrees of freedom d_{ij} of the χ distributions in the β-Laguerre random matrix are:

$$\mathbf{d} = \begin{bmatrix} n & & & & \\ \beta(m-1) & n-\beta & & & \\ & \beta(m-2) & n-2\beta & & \\ & & \beta(m-3) & n-3\beta & \\ & & & \ddots & \ddots \end{bmatrix}. \tag{D9}$$

We recall that in this case $n = m\beta\mathrm{e}^{A}$ is not the dimension of the matrix $\mathbf{R}$, which is an $m \times m$ square matrix, but a positive real number. Therefore, the rectangularity parameter does not need to be approximated in this method.

Figure 8 shows numerical results of the random-matrix estimates of the average entropy-production minimum for the 1D biased random walk with bias $A = 1$. We draw $m \times m$ random matrices from the $\beta = 1, 2, 1000$ Laguerre ensembles. Note that Laguerre ensembles of Dyson indices $\beta = 1, 2, 4$ are equivalent to Wishart random matrices with $\mathbf{R}_{ij}$ given respectively by real, complex and quaternionic normal random variables, and use the appropriate conjugate transpose of $\mathbf{R}$ [70]. We plot the maximum relative error $\epsilon_{\max}$ (D6) as a function of the size of the random matrix m (figure 8(a)). The Wishart (1-Laguerre) ensemble provides a biased overestimate of the real value with maximum relative error 2.3% for small random matrices of sizes larger than 64×64. We observe that the 2-Laguerre ensemble provides an estimate that is practically unbiased, even using small matrices (except in the limit $A \ll 1$). Furthermore, β-Laguerre matrices with large values of β (e.g. $\beta = 1000$) yield small dispersion in the relative difference but a bias (underestimation) for small matrix sizes. The mean and the standard deviation of $\epsilon_{\max}$ obtained from a large population of computer-generated random matrices are observed to converge to zero with the matrix size m as $\sim 1/m$. This fast convergence (compared to the usual $1/\sqrt{m}$) is a consequence of the correlation between the m eigenvalues of the β-Laguerre random matrices. The convergence of the estimates is revealed in the difference between the spectral density of the random matrices and the Marčenko–Pastur distribution for $m = 2^6$ (figure 8(b)) and $m = 2^{12}$ (figure 8(c)). Remarkably, even though for $m = 2^6$ the eigenvalue distribution is a rough approximation to the Marčenko–Pastur distribution, the relative error of the estimate is smaller than $\pm 2.3\%$ for a single 1-Laguerre and $\pm 1.5\%$ for a single 2-Laguerre random matrix.

Eventually, we notice that all the expressions that involve a sum over the eigenvalues can be recast into random matrix traces. For instance, the two minimum entropy estimates and their associated maximum relative error read:

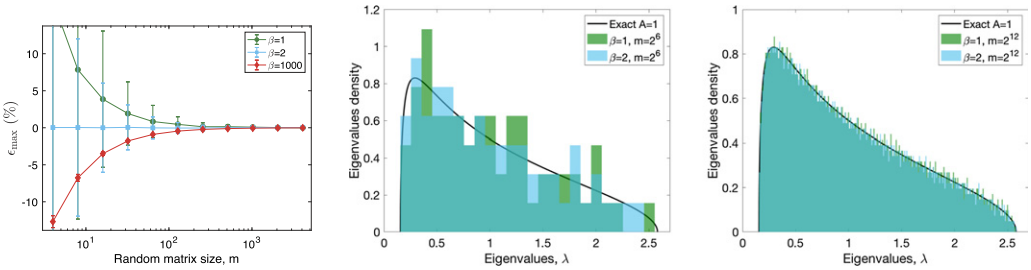

Figure 8. Numerical results for the random-matrix estimates $\langle \tilde{S}_{\min}(t)\rangle$ obtained using $m\times m$ random matrices drawn from the β-Laguerre ensemble. Left: average value of the maximum relative difference $\epsilon_{\max}$ given by equation (D6) as a function of the matrix size m obtained from $10^6/m$ random matrices, for three different $\beta-$Laguerre matrix ensembles (see legend). The error bars are given by the standard deviation of $\epsilon_{\max}$ across the random-matrix populations. Middle and right: normalized histograms for the eigenvalues of a single random matrix drawn from the β-Laguerre ensemble ($\beta = 1, 2$, see legend) with matrix sizes $m = 2^6$ (middle panel) and $m = 2^{12}$ (right panel), compared to the Marčenko–Pastur distribution (C1) with parameter $\delta = \mathrm{e}^{-A}$ (black line) and affinity $A = 1$.

$$\langle \tilde{S}_{\min}(t)\rangle_k = -Ak_- \int_0^t \frac{1}{m}\,\mathrm{Tr}\,\mathrm{e}^{-M\bar{k}t'}\,\mathrm{d}t', \tag{D10}$$

$$\langle \tilde{S}_{\min}(t)\rangle_\tau = \langle S_{\min}\rangle \left(1 - \frac{1}{m}\,\mathrm{Tr}\,\mathrm{e}^{-\mathbf{M}^{-1}t/\bar{\tau}}\right), \tag{D11}$$

$$\epsilon_{\max} = (1-\mathrm{e}^{-A})\frac{1}{m}\,\mathrm{Tr}\,\mathbf{M}^{-1} - 1, \tag{D12}$$

where $\mathbf{M}$ is either a Wishart random matrix or the Laguerre random matrix of size $m \times m$, scaled by $n = \mathrm{e}^A\beta m$ [see equations (D1) and (D7)].

Appendix E. Explicit expression for the average entropy production minimum

We now employ exact expressions for the moments of the Marčenko–Pastur distribution ρ to derive an analytical expression for the average minimum of the 1D biased random walk. The nth moment ($n \geqslant 1$) of the Marčenko–Pastur distribution $\rho(\lambda)$, can be expressed as power series of the parameter $\delta = \mathrm{e}^{-A}$ known as Narayana polynomials [77]:

$$\langle \lambda^n\rangle_\rho = \sum_{r=0}^{n-1} \binom{n}{r}\binom{n-1}{r}\frac{\delta^r}{r+1}. \tag{E1}$$

where $\langle \ldots\rangle_\rho$ denotes an average over the Marčenko–Pastur distribution (C1). Then, it is convenient to expand the exponential in equation (C6), and express the integrals in terms of the moments (E1). By manipulating the indices, we obtain two infinite series:

$$\langle S_{\min}(t)\rangle = A\ \mathrm{e}^{-A}\sum_{n=1}^{\infty}\frac{(-k_+t)^n}{n!}\langle \lambda^{n-1}\rangle_\rho \tag{E2}$$

$$= A\ \mathrm{e}^{-A}\left(-k_+t + (k_+t)^2\sum_{r=0}^{\infty}\sum_{s=0}^{\infty}\frac{(-k_+t)^{r+s}}{(r+s+2)!}\binom{r+s+1}{r}\binom{r+s}{r}\frac{\mathrm{e}^{-Ar}}{r+1}\right). \tag{E3}$$

This form can be identified as the *Kampé de Fériet* function F [94], a two-variable generalization of hypergeometric functions. It is defined for integer vectors $\mathbf{a}, b, b', c, d, d'$, of lengths p, q, q, r, s and s respectively, as follows:

$${}^{p+q}F_{r+s}\left[\begin{matrix}\mathbf{a}\ ,\ \mathbf{b}\ ,\ \mathbf{b}'\\ \mathbf{c}\ ,\ \mathbf{d}\ ,\ \mathbf{d}'\end{matrix}\middle|\, x\ ,\ y\right] \equiv \sum_{m=0}^{\infty}\sum_{n=0}^{\infty}\frac{\prod_{\alpha=1}^{p}(a_\alpha)_{m+n}\prod_{\beta=1}^{q}(b_\beta)_m(b'_\beta)_n}{\prod_{\gamma=1}^{r}(c_\gamma)_{m+n}\prod_{\delta=1}^{s}(d_\delta)_m(d'_\delta)_n}\frac{x^m y^n}{m!n!}\quad, \tag{E4}$$

where $(m)_n = \prod_{k=0}^{n-1}(m-k) = \frac{(m+n-1)!}{(m-1)!}$ denotes the rising factorial. The translations of the binomial coefficient into rising factorials yields the following expression of the mean minimum entropy:

$$\frac{\langle S_{\min}(t)\rangle}{A} = -k_-t + {}^{2+0}F_{1+1}\left[\begin{matrix}[2\ 1]\ ,\ \varnothing\ ,\ \varnothing\\ 3\ ,\ 2\ ,\ 2\end{matrix}\middle|\, -k_-t\ ,\ -k_+t\right]\frac{k_-k_+t^2}{2}. \tag{E5}$$

ORCID iDs

Edgar Roldán https://orcid.org/0000-0001-7196-8404
Frank Jülicher https://orcid.org/0000-0003-4731-9185

References

[1] Jülicher F, Ajdari A and Prost J 1997 Modeling molecular motors *Rev. Mod. Phys.* **69** 1269
[2] Howard J *et al* 2001 *Mechanics of Motor Proteins and the Cytoskeleton* (Sunderland, MA: Sinauer associates)
[3] Noji H, Yasuda R, Yoshida M and Kinosita K Jr 1997 Direct observation of the rotation of f1-atpase *Nature* **386** 299
[4] Bustamante C, Macosko J C and Wuite G J L 2000 Grabbing the cat by the tail: manipulating molecules one by one *Nat. Rev. Mol. Cell Biol.* **1** 130
[5] Schnitzer M J, Visscher K and Block S M 2000 Force production by single kinesin motors *Nat. Cell Biol.* **2** 718
[6] Ishii Y and Yanagida T 2000 Single molecule detection in life sciences *Single Mol.* **1** 5–16
[7] Helenius J, Brouhard G, Kalaidzidis Y, Diez S and Howard J 2006 The depolymerizing kinesin mcak uses lattice diffusion to rapidly target microtubule ends *Nature* **441** 115
[8] Ritort F 2006 Single-molecule experiments in biological physics: methods and applications *J. Phys.: Condens. Matter.* **18** R531
[9] Vogel S K, Pavin N, Maghelli N, Jülicher F and Tolić-Nørrelykke I M 2009 Self-organization of dynein motors generates meiotic nuclear oscillations *PLoS Biol.* **7** e1000087
[10] Aathavan K, Politzer A T, Kaplan A, Moffitt J R, Chemla Y R, Grimes S, Jardine P J, Anderson D L and Bustamante C 2009 Substrate interactions and promiscuity in a viral dna packaging motor *Nature* **461** 669
[11] Ananthanarayanan V, Schattat M, Vogel S K, Krull A, Pavin N and Tolić-Nørrelykke I M 2013 Dynein motion switches from diffusive to directed upon cortical anchoring *Cell* **153** 1526–36
[12] Fakhri N, Wessel A D, Willms C, Pasquali M, Klopfenstein D R, MacKintosh F C and Schmidt C F 2014 High-resolution mapping of intracellular fluctuations using carbon nanotubes *Science* **344** 1031–5
[13] Naganathan S R, Middelkoop T C, Fürthauer S and Grill S W 2016 Actomyosin-driven left-right asymmetry: from molecular torques to chiral self organization *Curr. Opinion Cell Biol.* **38** 24–30
[14] Ndlec F J, Surrey T, Maggs A C and Leibler S 1997 Self-organization of microtubules and motors *Nature* **389** 305
[15] Keller D and Bustamante C 2000 The mechanochemistry of molecular motors *Biophys. J.* **78** 541–56
[16] Qian H 2005 Cycle kinetics, steady state thermodynamics and motors-a paradigm for living matter physics *J. Phys.: Condens. Matter.* **17** S3783
[17] Klumpp S and Lipowsky R 2005 Cooperative cargo transport by several molecular motors *Proc. Natl Acad. Sci.* **102** 17284–9
[18] Campas O, Kafri Y, Zeldovich K, Casademunt J and Joanny J-F 2006 Collective dynamics of interacting molecular motors *Phys. Rev. Lett.* **97** 038101
[19] Kolomeisky A B and Fisher M E 2007 Molecular motors: a theorist's perspective *Annu. Rev. Phys. Chem.* **58** 675–95
[20] Brangwynne C P, Koenderink G H, MacKintosh F C and Weitz D A 2008 Cytoplasmic diffusion: molecular motors mix it up *J. Cell Biol.* **183** 583–7
[21] Gaspard P 2016 Template-directed copolymerization, random walks along disordered tracks, and fractals *Phys. Rev. Lett.* **117** 238101
[22] Sekimoto K 1997 Kinetic characterization of heat bath and the energetics of thermal ratchet models *J. Phys. Soc. Japan* **66** 1234–7
[23] Lau A, Lacoste D and Mallick K 2007 Nonequilibrium fluctuations and mechanochemical couplings of a molecular motor *Phys. Rev. Lett.* **99** 158102
[24] Chemla Y R, Moffitt J R and Bustamante C 2008 Exact solutions for kinetic models of macromolecular dynamics *J. Phys. Chem.* B **112** 6025–44
[25] Toyabe S, Okamoto T, Watanabe-Nakayama T, Taketani H, Kudo S and Muneyuki E 2010 Nonequilibrium energetics of a single f 1-atpase molecule *Phys. Rev. Lett.* **104** 198103
[26] Pietzonka P, Barato A C and Seifert U 2016 Universal bound on the efficiency of molecular motors *J. Stat. Mech.* 124004
[27] Hänggi P, Talkner P and Borkovec M 1990 Reaction-rate theory: fifty years after kramers *Rev. Mod. Phys.* **62** 251
[28] Qian H and Xie X S 2006 Generalized Haldane equation and fluctuation theorem in the steady-state cycle kinetics of single enzymes *Phys. Rev.* E **74** 010902
[29] Nishiyama M, Higuchi H and Yanagida T 2002 Chemomechanical coupling of the forward and backward steps of single kinesin molecules *Nat. Cell Biol.* **4** 790
[30] Carter N J and Cross R A 2005 Mechanics of the kinesin step *Nature* **435** 308
[31] Neri I, Roldán É and Jülicher F 2017 Statistics of infima and stopping times of entropy production and applications to active molecular processes *Phys. Rev.* X **7** 011019
[32] Gladrow J, Ribezzi-Crivellari M, Ritort F and Keyser U 2019 Experimental evidence of symmetry breaking of transition-path times *Nat. Commun.* **10** 55
[33] Peng C-K, Buldyrev S V, Goldberger A L, Havlin S, Sciortino F, Simons M and Stanley H E 1992 Long-range correlations in nucleotide sequences *Nature* **356** 168
[34] Arneodo A, Bacry E, Graves P V and Muzy J F 1995 Characterizing long-range correlations in dna sequences from wavelet analysis *Phys. Rev. Lett.* **74** 3293
[35] Bechhoefer J and Marshall B 2007 How xenopus laevis replicates dna reliably even though its origins of replication are located and initiated stochastically *Phys. Rev. Lett.* **98** 098105
[36] Godrèche C, Majumdar S N and Schehr G 2014 Universal statistics of longest lasting records of random walks and Lévy flights *J. Phys. A: Math. Theor.* **47** 255001
[37] Diffenbaugh N S, Pal J S, Trapp R J and Giorgi F 2005 Fine-scale processes regulate the response of extreme events to global climate change *Proc. Natl Acad. Sci.* **102** 15774–8
[38] Cheng L, AghaKouchak A, Gilleland E and Katz R W 2014 Non-stationary extreme value analysis in a changing climate *Climatic Change* **127** 353–69
[39] Novak S Y 2011 *Extreme Value Methods with Applications to Finance* (Boca Raton, FL: CRC Press)
[40] Rocco M 2014 Extreme value theory in finance: a survey *J. Econ. Surv.* **28** 82–108
[41] Brodin E and Klüppelberg C 2014 *Extreme Value Theory in Finance* (New York: Wiley)

[42] Noubary R D 2005 A procedure for prediction of sports records *J. Quant. Anal. Sports* **1** 1–14
[43] Einmahl J H J and Magnus J R 2008 Records in athletics through extreme-value theory *J. Am. Stat. Assoc.* **103** 1382–91
[44] Bittner E, Nußbaumer A, Janke W and Weigel M 2009 Football fever: goal distributions and non-Gaussian statistics *Eur. Phys. J.* B **67** 459–71
[45] Krug J 2007 Records in a changing world *J. Stat. Mech.* P07001
[46] Majumdar S N and Ziff R M 2008 Universal record statistics of random walks and Lévy flights *Phys. Rev. Lett.* **101** 050601
[47] Wergen G, Bogner M and Krug J 2011 Record statistics for biased random walks, with an application to financial data *Phys. Rev.* E **83** 051109
[48] Mounaix P, Majumdar S N and Schehr G 2018 Asymptotics for the expected maximum of random walks and Lévy flights with a constant drift *J. Stat. Mech.* 083201
[49] Godrèche C, Majumdar S N and Schehr G 2017 Record statistics of a strongly correlated time series: random walks and Lévy flights *J. Phys. A: Math. Theor.* **50** 333001
[50] Sabhapandit S 2019 Extremes and records (arXiv:1907.00944)
[51] Majumdar S N, Pal A and Schehr G 2020 Extreme value statistics of correlated random variables: a pedagogical review *Phys. Rep.* **840** 1–32
[52] Bénichou O, Krapivsky , Mejía-Monasterio C and Oshanin G 2016 Temporal correlations of the running maximum of a Brownian trajectory *Phys. Rev. Lett.* **117** 080601
[53] Hartich D and Godec A 2018 Duality between relaxation and first passage in reversible Markov dynamics: rugged energy landscapes disentangled *New J. Phys.* **20** 112002
[54] Hartich D and Godec A 2019 Interlacing relaxation and first-passage phenomena in reversible discrete and continuous space Markovian dynamics *J. Stat. Mech.* 024002
[55] Hartich D and Godec A 2019 Extreme value statistics of ergodic Markov processes from first passage times in the large deviation limit (arXiv:1902.00439)
[56] Chetrite R and Gupta S 2011 Two refreshing views of fluctuation theorems through kinematics elements and exponential martingale *J. Stat. Phys.* **143** 543
[57] Van Kampen N G 1992 *Stochastic Processes in Physics and Chemistry* vol 1 (Amsterdam: Elsevier)
[58] Bressloff P C 2014 *Stochastic Processes in Cell Biology* vol 41 (Berlin: Springer)
[59] Baiesi M and Maes C 2018 Life efficiency does not always increase with the dissipation rate *J. Phys. Commun.* **2** 045017
[60] Pigolotti S, Neri I, Roldán É and Jülicher F 2017 Generic properties of stochastic entropy production *Phys. Rev. Lett.* **119** 140604
[61] Redner S 2001 *A Guide to First-Passage Processes* (Cambridge: Cambridge University Press)
[62] Roldán É, Lisica A, Sánchez-Taltavull D and Grill S W 2016 Stochastic resetting in backtrack recovery by rna polymerases *Phys. Rev.* E **93** 062411
[63] Gingrich T R and Horowitz J M 2017 Fundamental bounds on first passage time fluctuations for currents *Phys. Rev. Lett.* **119** 170601
[64] Singh S, Menczel P, Golubev D S, Khaymovich I M, Peltonen J T, Flindt C, Saito K, Roldán É and Pekola J P 2019 Universal first-passage-time distribution of non-Gaussian currents *Phys. Rev. Lett.* **122** 230602
[65] Krapivsky P L and Redner S 2018 First-passage duality *J. Stat. Mech.* 093208
[66] Marčenko V A and Pastur L A 1967 Distribution of eigenvalues for some sets of random matrices *Mathematics USSR-Sbornik* **1** 457–83
[67] Nica A and Speicher R 2006 *Lectures on the Combinatorics of Free Probability* vol 13 (Cambridge: Cambridge University Press)
[68] Fridman M, Pugatch R, Nixon M, Friesem A A and Davidson N 2012 Measuring maximal eigenvalue distribution of Wishart random matrices with coupled lasers *Phys. Rev.* E **85** 020101
[69] Livan G, Novaes M and Vivo P 2018 *Introduction to Random Matrices: Theory and Practice* vol 26 (Berlin: Springer)
[70] Dumitriu I and Edelman A 2002 Matrix models for beta ensembles *J. Math. Phys.* **43** 5830–47
[71] Mainardi F and Spada G 2011 Creep, relaxation and viscosity properties for basic fractional models in rheology *Eur. Phys. J. Spec. Top.* **193** 133–60
[72] Tracy C A and Widom H 1994 Level-spacing distributions and the Airy Kernel *Commun. Math. Phys.* **159** 151–74
[73] Tracy C A and Widom H 1996 On orthogonal and symplectic matrix ensembles *Commun. Math. Phys.* **177** 727–54
[74] Brouwer P W, Frahm K M and Beenakker C W J 1997 Quantum mechanical time-delay matrix in chaotic scattering *Phys. Rev. Lett.* **78** 4737
[75] Prähofer M and Spohn H 2000 Universal distributions for growth processes in 1 + 1 dimensions and random matrices *Phys. Rev. Lett.* **84** 4882
[76] Dhar A, Kundu A, Majumdar S N, Sabhapandit S and Schehr G 2017 Exact extremal statistics in the classical 1D coulomb gas *Phys. Rev. Lett.* **119** 060601
[77] Dumitriu I and Rassart E 2003 Path counting and random matrix theory (arXiv: math/0307252)
[78] Redemann S *et al* 2017 Elegans chromosomes connect to centrosomes by anchoring into the spindle network *Nat. Commun.* **8** 15288
[79] Richard M, Blanch-Mercader C, Ennomani H, Cao W, De La Cruz E, Joanny J-F, Jülicher F, Blanchoin L and Martin P 2019 Active cargo positioning in antiparallel transport networks PNAS **116** 14835–42
[80] Harris R J and Schütz G M 2007 Fluctuation theorems for stochastic dynamics *J. Stat. Mech.* P07020
[81] Strasberg P, Schaller G, Lambert N and Brandes T 2016 Nonequilibrium thermodynamics in the strong coupling and non-Markovian regime based on a reaction coordinate mapping *New J. Phys.* **18** 073007
[82] Harris R and Shreshtha M 2019 Thermodynamic uncertainty for run-and-tumble type processes *Europhys. Lett.* **126** 40007
[83] Proesmans K, Toral R and Van den Broeck C 2019 Phase transitions in persistent and run-and-tumble walks *Phys.* A 121934
[84] Loos S A and Klapp S H 2019 Heat flow due to time-delayed feedback *Sci. Rep.* **9** 2491
[85] Oberreiter L, Seifert U and Barato A C 2019 Subharmonic oscillations in stochastic systems under periodic driving (arXiv:1902.01963)
[86] Polettini M and Esposito M 2017 Effective thermodynamics for a marginal observer *Phys. Rev. Lett.* **119** 240601
[87] Martínez I A, Bisker G, Horowitz J M and Parrondo J M 2019 Inferring broken detailed balance in the absence of observable currents *Nat. Commun.* **10** 1–10
[88] Skellam J G 1946 The frequency distribution of the difference between two Poisson variates belonging to different populations *J. R. Stat. Soc.* **109** 296
[89] Touchette H 2009 The large deviation approach to statistical mechanics *Phys. Rep.* **478** 1–69

[90] Speck T, Engel A and Seifert U 2012 The large deviation function for entropy production: the optimal trajectory and the role of fluctuations *J. Stat. Mech.* P12001
[91] Jarzynski C 1997 Nonequilibrium equality for free energy differences *Phys. Rev. Lett.* **78** 2690
[92] Seifert U 2005 Entropy production along a stochastic trajectory and an integral fluctuation theorem *Phys. Rev. Lett.* **95** 040602
[93] Neri I, Roldán E, Pigolotti S and Jülicher F 2019 Integral fluctuation relations for entropy production at stopping times (arXiv:1903.08115)
[94] Exton H 1978 *Handbook of Hypergeometric Integrals: Theory, Applications, Tables, Computer Programs* (Chichester, UK: Ellis Horwood)